modeling is accurate, the first excited state, which has $S = {}^5/_2$, is only 2.85 $cm^{-1}$ above the ground state. Magnetic fields as large as 230 kOe would lead to such an appreciable Zeeman splitting of the $S = {}^5/_2$ excited spin state that a component of this state becomes the ground state at high magnetic fields. In fact, magnetic anisotropy would lead to magnetic field mixing of the various spin states of **5**. Detailed magnetization studies of **5** are needed; however, it will also be necessary to characterize the relaxation time of the magnetization of **5** to decide whether the $Mn_9$ complexes in a crystal of **5** are behaving as a simple paramagnet or are exhibiting superparamagnetism or, for that matter, superantiferromagnetism.[36]

(36) Néel, L. *C. R. Hebd. Seances Acad. Sci.* **1961**, *252*, 4075-4080; *253*, 9-12; *253*, 203-208.

**Acknowledgment.** Funding from National Science Foundation Grant CHE-8507748 (G.C.) and partial funding from National Institutes of Health Grant HL13652 (D.N.H.) are gratefully acknowledged.

**Registry No. 5**, 112068-77-6; $Mn_3O(O_2CPh)_6(pyr)_2(H_2O)$, 109862-72-8.

**Supplementary Material Available:** Tables of anisotropic thermal parameters of manganese ions and all bond lengths and angles for complex **5** (7 pages); listing of calculated and observed structure factors (9 pages). Ordering information is given on any current masthead page. A complete MSC structure report (86109) is available on request from the Indiana University Chemistry library.

# Thermal Decarbonylation of Molybdenum(II) Carbonyl-Iodide Complexes. Molecular and Electronic Structures of the Mixed-Valence Trinuclear Clusters $Mo_3HI_7L_3$ (L = Tetrahydrofuran, Acetonitrile, Benzonitrile) and Molecular Structures of $MoI_3(EtCN)_3$ and $Mo_2I_4(PhCN)_4$

**F. Albert Cotton* and Rinaldo Poli*†**

*Contribution from the Department of Chemistry and Laboratory for Molecular Structure and Bonding, Texas A&M University, College Station, Texas 77843.* *Received July 30, 1987*

**Abstract:** Trinuclear cluster compounds of the type $Mo_3HI_7L_3$ (L = THF, $CH_3CN$, $C_6H_5CN$) can be obtained by decarbonylation of carbonyl-iodide complexes of molybdenum(II) in the presence of hard-donor ligands. In tetrahydrofuran (THF) an oligonuclear compound of stoichiometry $\{MoI_2(THF)_n\}_x$ (**1**) is formed as the main product. The trinuclear cluster $Mo_3HI_7(THF)_3 \cdot THF$ (**2**) is obtained from the same reaction in low yields. When MeCN and EtCN are used as solvents, solutions containing the quadruply bonded dimers $Mo_2I_4(RCN)_4$ are obtained, together with other minor insoluble products. Interaction of compound **1** with RCN also gives $Mo_2I_4(RCN)_4$, which is unstable toward loss of the nitrile and cannot be isolated for R = Me and Et. A ligand-exchange reaction with PhCN affords $Mo_2I_4(PhCN)_4$ (**6**), which is stable in the solid state. Other compounds that are produced in smaller yields in these reactions have been isolated and characterized, namely $Mo_3HI_7(MeCN)_3 \cdot MeCN$ (**3**), $MoI_3(EtCN)_3$ (**4**), and $Mo_3HI_7(PhCN)_3 \cdot C_6H_5CH_3$ (**5**). Compound **1** also reacts with $PMe_3$ to afford $Mo_2I_4(PMe_3)_4$ and with $I^-$ to produce the $[Mo_4I_{11}]^-$ anion. A different form of the trinuclear cluster with coordinated THF has also been obtained, $Mo_3HI_7(THF)_3$ (**7**). Crystal data are the following. Compound **2**: orthorhombic; space group *Pcam*; $a = 21.216$ (3), $b = 8.459$ (1), $c = 18.477$ (2) Å; $V = 3316$ (1) Å$^3$; $Z = 4$; $d_{calcd} = 2.933$ g·cm$^{-3}$; $R = 0.0461$, $R_w = 0.0743$ for 148 parameters and 1716 observed data [$F_o^2 > 3\sigma(F_o^2)$]. Compound **3**: orthorhombic; space group *Pcmb*; $a = 7.703$ (1), $b = 17.903$ (2), $c = 20.179$ (2) Å; $V = 2783$ (1) Å$^3$; $Z = 4$; $d_{calcd} = 3.199$ g·cm$^{-3}$; $R = 0.0355$, $R_w = 0.0478$ for 103 parameters and 1661 observations with $F_o^2 > 3\sigma(F_o^2)$. Compound **4**: monoclinic; space group $P2_1/n$; $a = 11.065$ (5), $b = 13.174$ (3), $c = 12.974$ (5) Å; $\beta = 103.70$ (3)°; $V = 1836$ (2) Å$^3$; $Z = 4$; $d_{calcd} = 2.321$ g·cm$^{-3}$; $R = 0.0570$, $R_w = 0.0680$ for 145 parameters and 1379 observations with $F_o^2 > 3\sigma(F_o^2)$. Compound **5**: monoclinic; space group $P2_1/m$; $a = 8.606$ (3), $b = 18.471$ (10), $c = 12.628$ (6) Å; $\beta = 96.38$ (4)°; $V = 1995$ (3) Å$^3$; $Z = 2$; $d_{calcd} = 2.626$ g·cm$^{-3}$; $R = 0.0495$, $R_w = 0.0728$ for 144 parameters and 1594 observations with $F_o^2 > 3\sigma(F_o^2)$. Compound **6**: orthorhombic; space group *Fddd*; $a = 22.941$ (2), $b = 39.516$ (12), $c = 17.336$ (8) Å; $V = 15715$ (15) Å$^3$; $Z = 16$; $d_{calcd} = 1.879$ g·cm$^{-3}$; $R = 0.0664$, $R_w = 0.0827$ for 92 parameters and 851 observations with $F_o^2 > 3\sigma(F_o^2)$. Compound **7**: trigonal; space group *R3m*; $a = 17.112$ (4), $c = 8.599$ (2) Å; $V = 2180.5$ (14) Å$^3$; $Z = 3$; $d_{calcd} = 4.158$ g·cm$^{-3}$; $R = 0.0428$, $R_w = 0.0583$ for 43 parameters and 321 observations with $F_o^2 > 3\sigma(F_o^2)$. The structure of the $Mo_3HI_7L_3$ (L = THF, MeCN, PhCN) clusters consists of an equilateral-triangular arrangement of the metals with strong metal-metal bonding interactions. The faces of the triangle are capped by an iodide and a hydride ligand, and a bridging iodide ion spans each edge. The structure is completed by three terminal iodide ions and three terminal ligands L. The $Mo_3I_7$ core of the molecules can be described as what would remain from the $Mo_6I_8$ cluster core found in $\alpha$-$MoI_2$, upon removal of a $(\mu_3\text{-I})Mo_3$ unit. The presence of H is inferred from the diamagnetism and the presence of an $^1H$ resonance at −10.31 ppm for compound **5**. A molecular orbital treatment of the trinuclear cluster with the Fenske-Hall method is presented.

Molybdenum and tungsten $MX_2$ (X = Cl, Br, I) compounds are known to exist as extended layered structures containing $[M_6X_8]^{4+}$ cores linked by additional $X^-$ ions, i.e. $\{[M_6X_8]X_2X_{4/2}\}_\infty$, at least in their crystalline form generally referred to as the $\alpha$-form. Structurally characterized examples are $MoCl_2$[1] and $MoI_2$,[2] while $W_6Br_{16}$ has also been shown[3] to contain $[W_6Br_8]^{4+}$ units bridged by $[Br_4]^{2-}$ anions. A water adduct of $MoBr_2$, $Mo_6Br_{12}(H_2O)_2$, has also been structurally characterized,[4] as well as the anions

† Present address: Department of Chemistry and Biochemistry, University of Maryland, College Park, MD 20742.

(1) Schäfer, H.; von Schnering, H.-G.; Tillack, J.; Kuhnen, F.; Wöhrle, H.; Baumann, H. *Z. Anorg. Allg. Chem.* **1967**, *353*, 281.
(2) Aliev, Z. G.; Klinkova, L. A.; Dubrovin, I. V.; Atovmyan, L. O.; *Russ. J. Inorg. Chem. Engl. Transl.* **1981**, *26*, 1060.
(3) Siepmann, R.; von Schnering, H.-G. *Z. Anorg. Allg. Chem.* **1968**, *357*, 289.

0002-7863/88/1510-0830$01.50/0 

**Scheme I**[a]

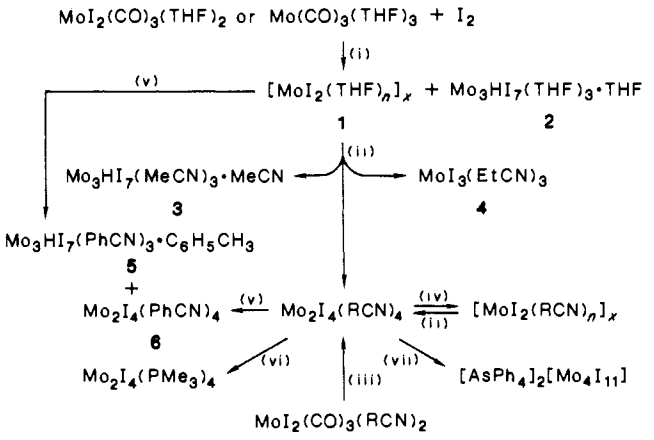


[a] Key: (i) reflux in THF; (ii) RCN (R = Me, Et), room temperature; (iii) RCN (R = Me, Et), reflux; (iv) evaporation; (v) PhCN, room temperature; (vi) $PMe_3$, room temperature; (vii) $I^-$ in THF, room temperature, then $AsPh_4Cl$.

$[W_6X_{14}]^{2-}$ (X = Cl, Br, I)[5] and the compounds $Mo_6Cl_{12}[P(n\text{-}Bu)_3]_2$,[6] $Mo_6Cl_{10}Et_2[P(n\text{-}Bu)_3]_2$,[6] and $W_6Cl_{12}[P(n\text{-}Bu)_3]_2$.[7] Numerous molecular orbital calculations have been carried out on clusters of this type.[8]

A number of other discrete clusters of these metals have been interpreted as fragments of the $[M_6X_8]^{4+}$ unit, the coordination spheres around the metals being completed by additional neutral or anionic ligands. Examples are the pentanuclear $\{[Mo_5Cl_8]Cl_5\}^{2-}$,[9] the tetranuclear $\{[Mo_4I_7]I_4\}^{2-}$,[10] and the tetranuclear $\{[Mo_4Cl_8]Cl_4\}^{3-}$ in both its isomeric (rectangular and butterfly) forms.[11]

We report here the isolation, characterization, and theoretical study of the first trinuclear clusters that can also be described as fragments of the octahedral $[M_6X_8]^{4+}$ core, i.e. $[Mo_3I_7](\mu_3\text{-}H)L_3$ [L = tetrahydrofuran (THF), MeCN, and PhCN],[12] that were obtained while decarbonylation processes of molybdenum(II) carbonyl–iodide complexes in the presence of hard-donor ligands were studied. Analogous decarbonylation processes in the presence of soft-donor ligands have been previously reported.[13] We will also describe some related chemistry (see Scheme I), including the formation in solution of the labile complexes $Mo_2I_4(RCN)_4$ (R = Me, Et) and the isolation and structural characterization of $MoI_3(EtCN)_3$ and $Mo_2I_4(PhCN)_4$.

## Experimental Section

All operations were performed under an atmosphere of prepurified argon with standard Schlenk-tube techniques. Solvents were purified by conventional methods and distilled under dinitrogen prior to use. Instruments used were as follows: IR, Perkin-Elmer 783; UV/visible, Cary 17; EPR, Varian E-6S; magnetic susceptibility, Johnson-Matthey. Variable-temperature magnetic measurements on $Mo_3HI_7(THF)_3$·THF were recorded on a superconducting SQUID susceptometer at Michigan State University. Elemental analyses were by Galbraith Laboratories, Knoxville, TN.

**Thermal Reaction of $Mo(CO)_3(\eta^6\text{-}C_6H_5CH_3)$ with $I_2$ in THF. Formation of $Mo_3HI_7(THF)_3$·THF.** $Mo(CO)_3(\eta^6\text{-}C_6H_5CH_3)$ (3.13 g, 11.50 mmol) was dissolved in 50 mL of THF, and the solution was stirred at room temperature for a few minutes. IR monitoring indicated that conversion to $Mo(CO)_3(THF)_3$ had occurred (bands at 1917 and 1775 $cm^{-1}$). $I_2$ (2.89 g, 11.37 mmol) was added, and the resulting solution was immediately warmed to the reflux temperature and stirred. After ca. 20 h the black solid that had formed (sample A) was filtered off, washed with THF, and dried in vacuo; yield 3.65 g. IR (Nujol mull, $cm^{-1}$): 1335 m, 1240 w, 1170 w, 1035 s, 1010 m, 920 m, 860 vs, 670 w. The solution from which this solid precipitated had a strong IR band at 1978 $cm^{-1}$ [$Mo(CO)_6$] plus others of an as yet unidentified compound at 1963 m, 1908 s, 1855 s, and 1840 m $cm^{-1}$. It was set aside at room temperature without stirring. Well-formed black crystals of $Mo_3HI_7(THF)_3$·THF formed over a few weeks. They were separated from the mother liquor, washed with THF, and vacuum dried; yield 86 mg. Anal. Calcd for $C_{16}H_{33}I_7Mo_3O_4$: C, 13.11; H, 2.26. Found: C, 12.85; H, 2.22. IR (Nujol mull, $cm^{-1}$): 1360 w, 1340 m, 1240 w, 1170 w, 1065 m, 1040 w, 1010 s, 920 w, 855 vs, 680 w. A single crystal from this batch was used for the X-ray analysis.

**Thermal Treatment of $Mo_2I_4(CO)_8$ in THF.** $Mo_2I_4(CO)_8$[14] (0.32 g, 0.35 mmol) was treated with THF (5 mL) and the resulting solution [of $MoI_2(CO)_3(THF)_2$[14]] immediately refluxed for ca. 20 h. The black precipitate that was formed (sample B) was filtered off, washed with THF, and dried in vacuo; yield 0.13 g. This had IR spectroscopic properties identical with those of sample A, obtained from $Mo(CO)_3(\eta^6\text{-}C_6H_5CH_3)$ and $I_2$ (vide supra). Anal. Calcd for $C_{12}H_{24}I_8Mo_4O_3$: C, 8.92; H, 1.50. Found: C, 8.89; H, 1.57. The same experiment was repeated with a longer reflux time (3 days), and the isolated solid gave the following analytical results: C, 9.48; H, 1.74. From the mother liquor of sample B black crystals formed over several days. Their IR spectroscopic properties and unit cell dimensions were identical with those of $Mo_3HI_7(THF)_3$·THF (vide supra).

**Reactions of Sample A with Nitriles. (a) Acetonitrile. Formation of $Mo_3HI_7(MeCN)_3$·MeCN.** A 0.34-g sample of A was suspended in 20 mL of MeCN and the mixture stirred at room temperature. Most of the solid dissolved to afford an emerald green solution, while a brown material remained undissolved. After subsequent reflux for ca. 2 h, the mixture was filtered while hot. Brown crystals of $Mo_3HI_7(MeCN)_3$·MeCN formed from the green filtrate upon cooling. One of these was used for the X-ray analysis. IR (Nujol mull, $cm^{-1}$): 2307 m, 2277 m (the peaks were calibrated with CO(g) on expanded abscissa). The mother liquor of these crystals was evaporated to dryness. The residue changed color to green-brown while it was dried at $5 \times 10^{-2}$ mmHg. Subsequent treatment with fresh MeCN restored the original olive green solution, whose UV/visible spectrum is shown in Figure 1 (after dilution in $CH_2Cl_2$).

**(b) Propionitrile. Formation of $MoI_3(EtCN)_3$.** A 0.84-g sample of A was treated with 10 mL of EtCN. A deep emerald green solution and some undissolved brown material were formed. The solution was filtered and reduced in volume by evaporation under reduced pressure to ca. 1 mL. This was treated with toluene (10 mL) and the resulting green solution filtered and layered with *n*-hexane. Slow diffusion of the two phases produced needle-shaped red crystals of $MoI_3(EtCN)_3$, one of which was used for the X-ray analysis. Their IR (Nujol mull) properties were identical with those of the undissolved material: 2278 m, 2270 m (these two peaks were calibrated with CO(g) on expanded abscissa), 1405 w, 1305 w, 1070 w, 790 w, 570 vw $cm^{-1}$. The mother liquor of these crystals had changed color from green to blue-green. An aliquot of this was diluted with $CH_2Cl_2$ (<1:10), and the UV/visible spectrum of the resulting solution is given in Figure 1. Attempts to isolate the blue-green material (presumably $Mo_2I_4(EtCN)_4$, see Discussion) out of this solution failed, as evaporation to dryness resulted in the production of a brown solid. The latter dissolved in dry EtCN to reafford the original blue-green solution.

**(c) Benzonitrile. Formation of $Mo_3HI_7(PhCN)_3$.** A 0.27-g sample of A was treated with PhCN (3 mL). A deep golden yellow solution and some undissolved brown material were formed. The solution was filtered and treated with 5 mL of toluene, followed by cooling to −20 °C. Very dark cube-shaped crystals of $Mo_3HI_7(PhCN)_3$·$C_6H_5CH_3$ formed in about

(4) Guggenberger, J.; Sleight, A. W. *Inorg. Chem.* **1969**, *8*, 2041.
(5) Zietlow, T. C.; Schaefer, W. P.; Sadeghi, B.; Hua, N.; Gray, H. B. *Inorg. Chem.* **1986**, *25*, 2195.
(6) Saito, T.; Nishida, M.; Yamagata, T.; Yamagata, Y.; Yamaguchi, Y. *Inorg. Chem.* **1986**, *25*, 1111.
(7) Saito, T.; Manabe, H.; Yamagata, T.; Imoto, H. *Inorg. Chem.* **1987**, *26*, 1362.
(8) (a) Cotton, F. A.; Haas, T. E. *Inorg. Chem.* **1964**, *3*, 10. (b) Bursten, B. E.; Cotton, F. A.; Stanley, G. G. *Isr. J. Chem.* **1980**, *19*, 132. (c) Woolley, R. G. *Inorg. Chem.* **1985**, *24*, 3519. (d) Hughbanks, T.; Hoffmann, R. *J. Am. Chem. Soc.* **1983**, *105*, 1150.
(9) Jödden, K.; von Schnering, H.-G.; Schäfer, H. *Angew. Chem., Int. Ed. Engl.* **1975**, *14*, 570.
(10) Stensvad, S.; Helland, B. J.; Babich, M. W.; Jacobson, R. A.; McCarley, R. E. *J. Am. Chem. Soc.* **1978**, *100*, 6257.
(11) Aufdembrink, B. A.; McCarley, R. E. *J. Am. Chem. Soc.* **1986**, *108*, 2474.
(12) A related trinuclear cluster, $[Mo_3(\mu_3\text{-}Cl)_2(\mu\text{-}Cl)_3Cl_6]^{2-}$, has also been recently communicated. Blatchford, T. P.; McCarley, R. E. *Abstracts of Papers*, 193rd National Meeting of the American Chemical Society, Denver, CO, April 5–10, 1987; American Chemical Society: Washington, DC, 1987; INOR 363.
(13) (a) Cotton, F. A.; Poli, R. *J. Am. Chem. Soc.* **1986**, *108*, 5628. (b) Cotton, F. A.; Poli, R. *Inorg. Chem.* **1986**, *25*, 3624. (c) Cotton, F. A.; Dunbar, K. R.; Poli, R. *Inorg. Chem.* **1986**, *25*, 3700. (d) Cotton, F. A.; Poli, R. *Inorg. Chem.* **1986**, *25*, 3703.
(14) (a) Poli, R. *Testi di Perfezionamento*; Scuola Normale Superiore: Pisa, 1985. (b) Calderazzo, F.; Poli, R.; Zanazzi, P. F. *Gazz. Chim. Ital.*, in press.

2 days; yield 0.03 g. IR (Nujol mull, $cm^{-1}$): 2245 m, 2230 sh, 1590 w, 1485 w, 1445 m, 1335 w, 1315 w, 1290 w, 1200 w, 1175 w, 1165 w, 1100 w, 1070 w, 1025 w, 1000 w, 935 w, 895 vw, 850 w, 760 s, 730 m, 685 s, 555 m, 470 w. $^1H$ NMR ($CH_2Cl_2$, $\delta$): 8.0 (m, aromatic), 2.34 (s, $CH_3$), −10.31 (s, $\mu_3$-H). Anal. Calcd for $C_{28}H_{23}I_7Mo_3N_3$: C, 21.30; H, 1.53; N, 2.66. Found: C, 21.82; H, 1.49; N, 3.35. One of these crystals was used for the X-ray analysis.

**Thermal Treatment of $Mo_2I_4(CO)_8$ with Propionitrile. Reactivity of the Resulting Solution.** Reflux of $Mo_2I_4(CO)_8$ in propionitrile (ca. 5 h) afforded a deep emerald green solution whose UV/visible properties were identical with those of the solution obtained by treating sample A with propionitrile (vide supra). This solution reacted with the following materials:

**(a) With $PMe_3$. Formation of $Mo_2I_4(PMe_3)_4$.** $Mo_2I_4(CO)_8$ (0.29 mg, 0.31 mmol) and propionitrile (5 mL) were reacted as described above. The filtered green solution was treated at room temperature with 0.5 mL (ca. 5 mmol) of $PMe_3$. The formation of a dark precipitate was observed. The mixture was evaporated to dryness and the residue recrystallized from hot hexane. Cooling of the filtered solution to −78 °C afforded 0.18 g of $Mo_2I_4(PMe_3)_4$ (57% yield), whose spectroscopic properties were identical with those of an authentic sample.[13a]

**(b) With PhCN. Formation of $Mo_2I_4(PhCN)_4$.** The emerald green solution obtained from $Mo_2I_4(CO)_8$ (0.20 g, 0.22 mmol) in 5 mL of EtCN as described above was evaporated to ca. 1 mL and treated with PhCN (0.5 mL). The color changed to yellow-green. Further evaporation of the more volatile nitrile yielded a golden yellow solution. A diluted aliquot of this in $CH_2Cl_2$ gave the UV/visible spectrum reported in Figure 1 for $Mo_2I_4(PhCN)_4$. The benzonitrile solution was treated with toluene (3 mL) and then with *n*-hexane (ca. 1 mL). A total of 0.07 g of $Mo_2I_4(PhCN)_4$ was obtained as orange-brown thin plates. One of these was used for the X-ray analysis. Their IR (Nujol mull, $cm^{-1}$) spectrum was very similar to that of $Mo_3HI_7(PhCN)_3 \cdot C_6H_5CH_3$ (vide supra): 2245 m, 1590 w, 1485 w, 1445 m, 1200 w, 1175 w, 1070 w, 1025 w, 1000 w, 760 s, 730 m, 685 s, 555 m. When the dried product was dissolved in neat $CH_2Cl_2$, a cloudy solution was obtained, which did not reproduce the UV/visible spectrum of $Mo_2I_4(PhCN)_4$ (Figure 1). When, however, the solid was redissolved in PhCN and the resulting solution diluted with $CH_2Cl_2$, the spectrum of $Mo_2I_4(PhCN)_4$ was again obtained.

**(c) With $I^-$. Formation of $[Mo_4I_{11}^-]$.** The green solution obtained from $Mo_2I_4(CO)_8$ (0.48 g, 0.52 mmol) in 10 mL of EtCN was evaporated to dryness, and the residue was treated at room temperature with ca. 0.2 g (excess) of anhydrous NaI in THF (10 mL). The resulting brown solution was treated with $AsPh_4Cl$ (0.25 g, 0.59 mmol), causing the formation of $(AsPh_4)_2[Mo_4I_{11}]$ as a brown microcrystalline solid. This was filtered off and recrystallized from $CH_2Cl_2$/THF; yield 0.37 g (55%). Anal. Calcd for $C_{48}H_{40}As_2I_{11}Mo_4$: C, 22.64; H, 1.58; As, 5.88. Found: C, 22.93; H, 1.59; As, 5.46.

**(d) Unsolvated $Mo_3HI_7(THF)_3$.** A green solution obtained by refluxing 0.31 g (0.33 mmol) of $Mo_2I_4(CO)_8$ in propionitrile as described above was evaporated to dryness, and the residue was treated with $PPh_3$ (0.18 g, 0.70 mmol) in THF (20 mL). A yellow-brown solution was slowly obtained upon stirring at room temperature. The mixture was then gently refluxed, and a red solution was obtained. After filtration, toluene was carefully layered on top of the solution, causing the formation of a few needle-shaped crystals within a few days. These were shown to be of $Mo_3HI_7(THF)_3$ by X-ray analysis.

**X-ray Crystallography. (a) $Mo_3HI_7(THF)_3 \cdot THF$.** A cuboid-shaped crystal was glued to the tip of a glass fiber and mounted on a computer-controlled Rigaku AFC5R diffractometer equipped with a rotating-anode X-ray source. Data collection was routine. Pertinent crystal data are reported in Table I. An average 35.2% decay was observed in the three intensity standard reflections that were periodically monitored during the 8.5 h of data collection. The data were corrected for Lorentz–polarization effects, for decay, and for absorption.[15] The structure was solved by the SHELXS-86[16] direct-methods program, which showed the entire heavy-atom portion of the molecule. On the basis of systematic absences, the space group could be either $Pca2_1$ or *Pcam*. The noncentrosymmetric choice gave a plausible solution, which appeared to refine successfully. However, high correlation was present between all the pairs of variables related by the approximate mirror plane passing through the Mo1, I1, O1, and I22 atoms. Such a mirror plane was then imposed crystallographically by changing the space group to *Pcam*, and successful refinement was again achieved. The mirror plane imposes statistical disorder on the THF molecule that is bonded to Mo1. An additional absorption correction was performed[17] at the end of the isotropic refinement. Most of the oxygen and carbon atoms were refined isotropically, as an attempt to treat them anisotropically led to nonpositive definite tensors. Fractional atomic coordinates are listed in Table II, and selected bond distances and angles are reported in Table III.

**(b) $Mo_3HI_7(MeCN)_3 \cdot MeCN$.** A single crystal was glued to the tip of a glass fiber and mounted on the diffractometer. Data collection and reduction were performed as for $Mo_3HI_7(THF)_3 \cdot THF$ (vide supra). No correction for decay was necessary. Corrections for absorption were applied as for $Mo_3HI_7(THF)_3 \cdot THF$.[15,17] According to the systematic absences from the data, the space group could be either $Pc2_1b$ or *Pcmb*. By analogy with the THF adduct described above, the centrosymmetric space group was chosen and proved to be correct by the successful refinement. Table I contains crystal data, and fractional atomic coordinates are listed in Table IV, while Table III shows selected bond distances and angles.

**(c) $Mo_3HI_7(PhCN)_3 \cdot C_6H_5CH_3$.** A single crystal was sealed under argon in a thin-walled glass capillary and mounted on the diffractometer. Significant crystal data are assembled in Table I. Data collection (which occurred without decay) and reduction were routine. The data were corrected for absorption.[15] The structure was solved by direct methods in the space group $P2_1/m$, which then proved to be correct by the successful refinement. At the end of the refinement for the trinuclear cluster ($R = 0.061$), a disordered interstitial toluene molecule was found around an inversion center in the difference Fourier map. The disorder is schematically illustrated below.

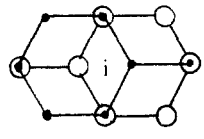


Inclusion of this model with the appropriate site occupancy factor for each carbon atom led to successful refinement and lowered the *R* factor to 0.046. Fractional atomic coordinates are reported in Table V, while selected bond distances and angles are listed in Table III.

**(d) $Mo_3HI_7(THF)_3$.** A single crystal was glued to the tip of a glass fiber and mounted on the diffractometer. Crystal data are reported in Table I. The data collection and reduction were routine. A semiempirical absorption correction[15] was applied according to the method described by North et al. The structure solution presented a few problems. According to the systematic absences from the data, the space group could be either *R*32, *R*3*m*, or *R*3*m*. Direct methods gave an octahedral arrangement of heavy atoms in each space group, with distances of 2.55 Å within each triangle and 2.8–2.9 Å between atoms of different triangles. This could be consistent with an octahedral arrangement of molybdenum atoms as found, for example, in $\alpha$-$MoI_2$.[2] This model, however, did not develop properly in any of the possible space groups. The Patterson map interpretation program of SHELXS-86[16] failed too. The breakthrough came when it was realized that the Patterson map, although consistent with the direct-methods solution, could also be in agreement with the structure found for the molybdenum–iodide trimers described above, $Mo_3HI_7L_3$ (L = THF, MeCN, PhCN), with the capping iodine atom lying on the threefold axis. Such a structure could be accommodated only in the *R*3*m* space group, and the introduction of the $Mo_3I_7$ model with the geometry calculated from the aforementioned $Mo_3HI_7L_3$ structures gave an isotropic refinement converging at $R = 0.20$. A difference Fourier analysis revealed the oxygen atom, and subsequent anisotropic refinement lowered the *R* factor to 0.065. The rest of the THF molecule was found to be disordered, although in a way different from that found in $Mo_3HI_7(THF)_3 \cdot THF$. The introduction of the carbon atoms as found in the difference Fourier map led to instability, which can be attributed to the spreading of the electron density as a result of the disorder and the high thermal motion. To correct this problem, the interatomic distances and angles of the THF molecule were restrained to the values obtained from the $Mo_3HI_7(THF)_3 \cdot THF$ structure and from the literature.[18] Refinement with the SHELX software of this model gave a final agreement factor $R = 0.0422$ ($R_w = 0.0583$). Fractional atomic coordinates are listed in Table VI, while selected bond distances and angles are reported in Table III.

**(e) *mer*-$MoI_3(EtCN)_3$.** A single crystal was sealed under argon in a thin-walled glass capillary and mounted on the diffractometer. Crystal data are assembled in Table I. Data collection and reduction were routine. A correction for decay (6.5% over the 36 h of data collection) and a semiempirical absorption correction[15] were applied. The structure was solved by direct methods and refined by full-matrix least-squares

(15) North, A. C. T.; Phillips, D. C.; Mathews, F. S. *Acta Crystallogr., Sect. A: Found. Crystallogr.* **1986**, *A24*, 351.
(16) Sheldrick, G. M. *SHELXS-86*; Institut für Anorganische Chemie der Universtat: Göttingen, F.R.G., 1986.
(17) Walker, N.; Stuart, D. *Acta Crystallogr., Sect. A: Found. Crystallogr.* **1983**, *A39*, 158.
(18) Cotton, F. A.; Poli, R. *Inorg. Chem.* **1987**, *26*, 1514.

**Table I.** Crystal Data for All Compounds

| compound | **2** | **3** | **4** | **5** | **6** | **7** |
|---|---|---|---|---|---|---|
| formula | $C_{16}H_{32}I_7Mo_3O_4$ | $C_8H_{12}I_7Mo_3N_4$ | $C_9H_{15}I_3MoN_3$ | $C_{28}H_{23}I_7Mo_3N_3$ | $C_{28}H_{20}I_4Mo_2N_4$ | $C_{12}H_{24}I_7Mo_3O_3$ |
| formula wt | 1464.58 | 1340.36 | 641.89 | 1577.66 | 1111.99 | 1392.47 |
| space grp | *Pcam*[a] | *Pcmb*[a] | $P2_1/n$ | $P2_1/m$ | *Fddd* | *R3m* |
| systematic absences | *h0l*: $h \neq 2n$ | *0kl*: $l \neq 2n$ | *0k0*: $k \neq 2n$ | *0k0*: $k \neq 2n$ | *hkl*: $h + k \neq 2n$, $h + l \neq 2n$, $k + l \neq 2n$; *hk0*: $h + k \neq 4n$; *h0l*: $h + l \neq 4n$; *0kl*: $k + l \neq 4n$ | *hkl*: $-h + k + l \neq 3n$ |
| | *0kl*: $l \neq 2n$ | *hk0*: $k \neq 2n$ | *h0l*: $h + l \neq 2n$ | | | |
| $a$, Å | 21.216 (3) | 7.703 (1) | 11.065 (5) | 8.606 (3) | 22.941 (5) | 17.112 (4) |
| $b$, Å | 8.459 (1) | 17.903 (2) | 13.174 (3) | 18.471 (10) | 39.516 (12) | 17.112 (4) |
| $c$, Å | 18.477 (2) | 20.179 (2) | 12.974 (5) | 12.628 (6) | 17.336 (8) | 8.599 (2) |
| $\alpha$, deg | 90 | 90 | 90 | 90 | 90 | 90 |
| $\beta$, deg | 90 | 90 | 103.70 (3) | 96.38 (4) | 90 | 90 |
| $\gamma$, deg | 90 | 90 | 90 | 90 | 90 | 120 |
| $V$, Å$^3$ | 3316 (1) | 2783 (1) | 1837 (2) | 1995 (3) | 15 715 (15) | 2180.5 (14) |
| $Z$ | 4 | 4 | 4 | 2 | 16 | 3 |
| $d_{calcd}$, g·cm$^{-1}$ | 2.933 | 3.199 | 2.321 | 2.626 | 1.879 | 4.158 |
| cryst size, mm | 0.5 × 0.5 × 0.5 | 0.05 × 0.1 × 0.4 | 0.1 × 0.3 × 0.6 | 0.3 × 0.4 × 0.5 | 0.05 × 0.4 × 0.4 | 0.1 × 0.1 × 0.3 |
| $\mu$(Mo K$\alpha$), cm$^{-1}$ | 75.635 | 89.92 | 56.745 | 62.917 | 37.535 | 118.262 |
| data collcn instrument | Rigaku AFC5R | CAD-4 | CAD-4 | Rigaku AFC5R | CAD-4 | CAD-4 |
| radiatn (monochromated in incident beam) | Mo K$\alpha$ ($\lambda_\alpha$ = 0.71073 Å) | | | | | |
| orientation reflcns: no., range ($2\theta$) | 25, 35–50 | 25, 16–30 | 25, 20–32 | 25, 18–25 | 25, 10–25 | 25, 10–32 |
| temp, °C | 20 | 20 | 20 | 20 | 20 | 20 |
| scan method | $\omega$–$2\theta$ | $\omega$ | $\omega$–$2\theta$ | $\omega$–$2\theta$ | $\omega$ | $\omega$ |
| data collcn range ($2\theta$), deg | 4–50 | 4–50 | 4–50 | 4–45 | 4–45 | 4–50 |
| no. unique data, total with $F_o^2 > 3\sigma(F_o^2)$ | 3347, 1716 | 2199, 1661 | 3226, 1379 | 2141, 1594 | 2580, 851 | 479, 321 |
| no. param refined | 148 | 103 | 145 | 144 | 92 | 43 |
| transmissn factors: max, min | 1.000, 0.479 | 1.00, 0.524 | 1.000, 0.314 | 1.000, 0.519 | 1.000, 0.554 | 0.998, 0.574 |
| $R$[b] | 0.0461 | 0.0355 | 0.0570 | 0.0495 | 0.0664 | 0.0428 |
| $R_w$[c] | 0.0743 | 0.0478 | 0.0680 | 0.0728 | 0.0827 | 0.0583 |
| quality of fit indicator[d] | 1.506 | 1.181 | 1.646 | 1.690 | 1.700 | 1.281 |
| largest shift/esd, final cycle | 0.34 | 0.14 | 0.15 | 0.27 | 0.04 | 0.20 |
| largest peak, e/Å | 1.241 | 1.219 | 0.979 | 1.154 | 1.63 | 1.28 |

[a] Nonstandard setting for *Pbcm* (No. 57). [b] $R = \sum||F_o| - |F_c||/\sum|F_o|$. [c] $R_w = [\sum w(|F_o| - |F_c|)^2/\sum w|F_o|^2]^{1/2}$; $w = 1/\sigma^2(|F_o|)$. [d] Quality of fit = $[\sum w(|F_o| - |F_c|)^2/(N_{obsd} - N_{param})]^{1/2}$.

**Table II.** Positional Parameters and Their Estimated Standard Deviations for $Mo_3HI_7(THF)_3 \cdot THF$[a]

| atom | $x$ | $y$ | $z$ | $B$, Å$^2$ |
|---|---|---|---|---|
| I1 | 0.3799 (1) | 0.3656 (2) | 0.250 | 4.58 (5) |
| I2 | 0.56106 (7) | 0.3567 (2) | 0.36905 (8) | 3.70 (3) |
| I12 | 0.42663 (7) | 0.6712 (2) | 0.40033 (8) | 3.83 (3) |
| I22 | 0.65455 (8) | 0.6540 (2) | 0.250 | 3.26 (4) |
| I122 | 0.50437 (9) | 0.9369 (2) | 0.250 | 3.05 (4) |
| Mo1 | 0.4342 (1) | 0.6523 (3) | 0.250 | 2.50 (5) |
| Mo2 | 0.53668 (7) | 0.6482 (2) | 0.31785 (8) | 2.34 (3) |
| O1 | 0.340 (1) | 0.781 (2) | 0.250 | 4.5 (5) |
| O2 | 0.5833 (7) | 0.774 (1) | 0.4096 (7) | 4.0 (3) |
| C11 | 0.330 (2) | 0.946 (5) | 0.250 | 22 (4) |
| C12 | 0.260 (3) | 0.962 (7) | 0.215 (3) | 8 (2)* |
| C13 | 0.233 (2) | 0.833 (5) | 0.250 | 9 (1) |
| C14 | 0.281 (1) | 0.703 (4) | 0.250 | 8 (1) |
| C21 | 0.580 (1) | 0.722 (3) | 0.486 (1) | 6.6 (7) |
| C22 | 0.603 (2) | 0.857 (3) | 0.527 (1) | 8.5 (9) |
| C23 | 0.638 (1) | 0.961 (3) | 0.477 (1) | 6.4 (7) |
| C24 | 0.617 (2) | 0.924 (3) | 0.406 (2) | 8.4 (8) |
| O3 | 0.250 | 0.379 (4) | 0.500 | 10 (1) |
| C31 | 0.248 (1) | 0.479 (4) | 0.565 (1) | 7.2 (8) |
| C32 | 0.259 (1) | 0.651 (3) | 0.540 (2) | 7.8 (8) |

[a] Starred values indicate atoms refined isotropically. Anisotropically refined atoms are given in the form of the equivalent isotropic displacement parameter defined as $^4/_3[a^2B_{11} + b^2B_{22} + c^2B_{33} + ab(\cos\gamma)B_{12} + ac(\cos\beta)B_{13} + bc(\cos\alpha)B_{23}]$.

cycles as for the structures described above. Hydrogen atoms were not included. An additional absorption correction[17] was applied at the end of the isotropic refinement. Fractional atomic coordinates are listed in Table VII, while selected bond distances and angles are reported in Table VIII.

**(f) $Mo_2I_4(PhCN)_4$.** The crystal was protected under argon in a sealed thin-walled glass capillary. Crystal data are presented in Table I. Data collection and reduction were performed in a routine manner, and the structure solution and refinement were carried out as described for the previous compounds. Corrections for absorption were applied.[15,17] Because of the limited number of data, only the heavy atoms (Mo and I) were refined anisotropically. Fractional atomic coordinates are reported in Table IX, and selected bond distances and angles are listed in Table X.

**Theoretical Calculations.** The Fenske–Hall[19a] molecular orbital treatment was employed on the model compounds $Mo_3I_7L_3$ and $Mo_3HI_7L_3$ (L = $H_2O$, HCN). The atomic 1s, 2s, 2p, 3s, 3p, 3d, 4s, and 4p orbitals of the I and Mo atoms and the 1s orbitals of the O, N, and C atoms were treated as "core". Atomic parameters from the $Mo_3HI_7(THF)_3$ and $Mo_3HI_7(MeCN)_3$ crystal structures idealized to $C_{3v}$ symmetry were employed, and a right-handed coordinate system was chosen, with the $z$ axis pointing from the center of the $Mo_3$ triangle toward the capping iodine atom. The hydrogen atom was introduced on the threefold axis in such a way that each Mo–H bond is collinear with the corresponding

(19) (a) Hall, M. B.; Fenske, R. F. *Inorg. Chem.* **1972**, *11*, 768. (b) Pauling, L. *The Nature of the Chemical Bond*, 3rd ed.; Cornell University: Ithaca, NY, 1960; p 226, 256.

**Table III.** Selected Bond Distances (Å) and Angles (deg) for the Compounds $Mo_3HI_7L_3$·L (L = THF, **2**; MeCN, **3**), $Mo_3HI_7(PhCN)_3$·$C_6H_5CH_3$ (**5**), and $Mo_3HI_7(THF)_3$ (**7**)

| | 2 | 3 | 5 | 7 | |
|---|---|---|---|---|---|
| | | | (a) Bond Distances | | |
| Mo(1)-Mo(2) | 2.509 (2) | 2.541 (1) | 2.525 (3) | Mo-Mo′ | 2.487 (4) |
| Mo(2)-Mo(2′) | 2.507 (2) | 2.539 (1) | 2.527 (3) | | |
| Mo(1)-I(122) | 2.830 (3) | 2.789 (2) | 2.805 (3) | Mo-I | 2.824 (2) |
| Mo(2)-I(122) | 2.830 (2) | 2.795 (1) | 2.826 (2) | | |
| Mo(1)-I(12) | 2.787 (2) | 2.790 (1) | 2.790 (2) | Mo-I(B) | 2.777 (3) |
| Mo(2)-I(12) | 2.795 (2) | 2.786 (1) | 2.771 (2) | | |
| Mo(2)-I(22) | 2.798 (2) | 2.806 (1) | 2.785 (2) | | |
| Mo(1)-I(1) | 2.685 (3) | 2.715 (2) | 2.674 (4) | Mo-I(T) | 2.692 (4) |
| Mo(2)-I(2) | 2.691 (2) | 2.706 (1) | 2.672 (2) | | |
| Mo(1)-L(1) | 2.27 (2) | 2.183 (14) | 2.22 (2) | Mo-O | 2.19 (4) |
| Mo(2)-L(2) | 2.232 (14) | 2.202 (9) | 2.15 (2) | | |
| | | | (b) Bond Angles | | |
| Mo(2)-Mo(1)-Mo(2′) | 59.95 (7) | 59.95 (4) | 60.04 (8) | Mo′-Mo-Mo″ | 60 |
| Mo(1)-Mo(2)-Mo(2′) | 60.03 (6) | 60.03 (3) | 59.98 (6) | | |
| Mo(1)-I(122)-Mo(2) | 52.64 (6) | 54.14 (3) | 53.28 (6) | Mo-I-Mo′ | 52.25 (8) |
| Mo(2)-I(122)-Mo(2′) | 52.60 (5) | 54.04 (3) | 53.11 (6) | | |
| Mo(1)-I(12)-Mo(2) | 53.43 (6) | 54.22 (4) | 54.02 (7) | Mo-I(B)-Mo′ | 53.2 (1) |
| Mo(2)-I(22)-Mo(2′) | 53.24 (6) | 53.81 (3) | 53.95 (6) | | |
| I(1)-Mo(1)-I(122) | 173.7 (1) | 177.95 (7) | 175.8 (1) | I(T)-Mo-I | 173.7 (1) |
| I(2)-Mo(2)-I(122) | 173.29 (7) | 175.56 (4) | 175.41 (9) | | |
| I(1)-Mo(1)-I(12) | 91.55 (5) | 91.54 (3) | 91.98 (6) | I(T)-Mo-I(B) | 91.1 (1) |
| I(2)-Mo(2)-I(12) | 91.88 (6) | 92.23 (4) | 91.59 (7) | | |
| I(2)-Mo(2)-I(22) | 90.12 (7) | 91.62 (4) | 91.67 (7) | | |
| I(1)-Mo(1)-L(1) | 93.3 (5) | 92.6 (4) | 94.1 (7) | I(T)-Mo-O | 97 (1) |
| I(2)-Mo(2)-L(2) | 94.8 (3) | 93.8 (2) | 97.0 (5) | | |
| I(12)-Mo(1)-I(12′) | 170.6 (1) | 171.40 (6) | 171.3 (1) | I(B)-Mo-I(B′) | 171.4 (2) |
| I(12)-Mo(2)-I(22) | 171.79 (7) | 170.49 (4) | 170.74 (9) | | |
| I(12)-Mo(1)-I(122) | 88.94 (5) | 88.60 (3) | 88.31 (6) | I(B)-Mo-I | 89.4 (1) |
| I(12)-Mo(2)-I(122) | 88.80 (6) | 88.57 (4e | 88.27 (6) | | |
| I(22)-Mo(2)-I(122) | 90.15 (7) | 88.26 (4) | 89.17 (7) | | |
| I(12)-Mo(1)-L(1) | 85.51 (5) | 85.92 (3) | 86.01 (6) | I(B)-Mo-O | 85.7 (8) |
| I(12)-Mo(2)-L(2) | 85.6 (4) | 84.4 (3) | 85.5 (5) | | |
| I(22)-Mo(2)-L(2) | 86.3 (4) | 86.7 (3) | 85.5 (5) | | |
| I(122)-Mo(1)-L(1) | 93.0 (5) | 89.5 (4) | 90.0 (7) | I-Mo-O | 90 (1) |
| I(122)-Mo(2)-L(2) | 91.9 (3) | 90.6 (2) | 87.6 (5) | | |

**Table IV.** Positional Parameters and Their Estimated Standard Deviations for $Mo_3HI_7(MeCN)_3$·MeCN[a]

| atom | x | y | z | B, Å² |
|---|---|---|---|---|
| I1 | 0.7325 (2) | 0.750 | 0.63934 (6) | 4.14 (3) |
| I2 | 0.73296 (9) | 0.88019 (4) | 0.43192 (5) | 4.18 (2) |
| I12 | 0.4034 (1) | 0.90541 (4) | 0.58079 (4) | 4.06 (2) |
| I22 | 0.3928 (2) | 0.750 | 0.34154 (6) | 4.15 (2) |
| I122 | 0.1140 (1) | 0.750 | 0.50284 (6) | 3.48 (2) |
| Mo1 | 0.4242 (2) | 0.750 | 0.57413 (7) | 2.68 (3) |
| Mo2 | 0.4216 (1) | 0.82091 (5) | 0.46504 (5) | 2.68 (2) |
| N1 | 0.276 (2) | 0.750 | 0.6663 (7) | 4.4 (3) |
| N2 | 0.273 (1) | 0.9135 (5) | 0.4211 (5) | 4.4 (2) |
| C1 | 0.204 (2) | 0.750 | 0.7149 (9) | 4.8 (4) |
| C2 | 0.100 (3) | 0.750 | 0.778 (1) | 8.6 (7) |
| C3 | 0.198 (1) | 0.9662 (6) | 0.4063 (7) | 4.5 (3) |
| C4 | 0.099 (2) | 1.0327 (7) | 0.3854 (8) | 5.8 (3) |
| N3 | −0.484 (7) | 1.000 | 0.250 | 28 (2)* |
| C5 | −0.336 (8) | 1.000 | 0.250 | 29 (3)* |
| C6 | −0.166 (5) | 1.000 | 0.250 | 14 (1)* |

[a] Starred values indicate atoms refined isotropically. Anisotropically refined atoms are given in the form of the isotropic equivalent displacement parameter defined as $^4/_3[a^2B_{11} + b^2B_{22} + c^2B_{33} + ab(\cos\gamma)B_{12} + ac(\cos\beta)B_{13} + bc(\cos\alpha)B_{23}]$.

**Table V.** Positional Parameters and Their Estimated Standard Deviations for $Mo_3HI_7(PhCN)_3$·$C_6H_5CH_3$[a]

| atom | x | y | z | B, Å² |
|---|---|---|---|---|
| I1 | −0.2577 (3) | 0.750 | −0.1836 (2) | 6.59 (6) |
| I2 | −0.2094 (2) | 0.8750 (1) | 0.1335 (1) | 6.17 (4) |
| I12 | −0.5424 (2) | 0.59941 (8) | −0.0996 (1) | 5.08 (3) |
| I22 | −0.4821 (3) | 0.750 | 0.2820 (1) | 5.04 (5) |
| I122 | −0.7839 (2) | 0.750 | 0.0235 (2) | 4.48 (5) |
| Mo1 | −0.5211 (3) | 0.750 | −0.0896 (2) | 3.62 (5) |
| Mo2 | −0.4941 (2) | 0.8184 (1) | 0.0847 (1) | 3.57 (4) |
| N1 | −0.676 (3) | 0.750 | −0.242 (2 | 6.5 (8) |
| N2 | −0.622 (2) | 0.902 (1) | 0.156 (1) | 5.2 (4) |
| C1 | −0.749 (4) | 0.750 | −0.328 (2) | 6.0 (9) |
| C2 | −0.711 (3) | 0.940 (1) | 0.187 (1) | 4.6 (5) |
| C10 | −0.846 (3) | 0.750 | −0.424 (2) | 4.3 (6)* |
| C11 | −0.782 (5) | 0.750 | −0.513 (3) | 8 (1)* |
| C12 | −0.877 (4) | 0.750 | −0.605 (3) | 7 (1)* |
| C13 | −1.036 (4) | 0.750 | −0.606 (2) | 6.0 (8)* |
| C14 | −1.098 (6) | 0.750 | −0.514 (4) | 11 (1)* |
| C15 | −0.997 (5) | 0.750 | −0.419 (3) | 8 (1)* |
| C20 | −0.830 (2) | 0.986 (1) | 0.226 (2) | 4.4 (4)* |
| C21 | −0.869 (3) | 0.972 (2) | 0.319 (2) | 8.7 (8)* |
| C22 | −0.997 (4) | 1.011 (2) | 0.358 (3) | 12 (1)* |
| C23 | −1.046 (4) | 1.065 (2) | 0.288 (3) | 13 (1)* |
| C24 | −1.007 (4) | 1.087 (2) | 0.203 (2) | 10 (1)* |
| C25 | −0.888 (3) | 1.041 (2) | 0.160 (2) | 7.9 (7)* |
| C100 | 0.484 (8) | 0.460 (3) | 0.482 (5) | 9 (2)* |
| C101 | 0.446 (4) | 0.497 (2) | 0.583 (2) | 9.5 (8)* |
| C102 | 0.487 (7) | 0.563 (4) | 0.601 (4) | 9 (2)* |
| C103 | 0.426 (5) | 0.398 (2) | 0.469 (3) | 14 (1)* |
| C104 | 0.391 (7) | 0.442 (4) | 0.549 (5) | 11 (2)* |

[a] Starred values indicate atoms refined anisotropically. Anisotropically refined atoms are given in the form of the equivalent isotropic displacement parameter defined as $^4/_3[a^2B_{11} + b^2B_{22} + c^2B_{33} + ab(\cos\gamma)B_{12} + ac(\cos\beta)B_{13} + bc(\cos\alpha)B_{23}]$.

trans Mo–L bond. The resulting Mo–H distance is 1.60 Å, which corresponds to the sum of the covalent radii for Mo and H.[19b] The local coordinate system for the metal atoms was chosen as follows: The $z$ axis on each molybdenum atom points toward the center of the $Mo_3$ triangle, the $x$ axis lies in the plane of the triangle, and the $y$ axis completes a right-handed coordinate system.

## Results and Discussion

The main interest of this study resides in the formation, the structure, and the electronic properties of the new class of trinuclear molybdenum clusters, $Mo_3HI_7L_3$ (L = neutral mono-

**Table VI.** Positional Parameters and Their Estimated Standard Deviations for $Mo_3HI_7(THF)_3$[a]

| atom | x | y | z | B, Å² |
|---|---|---|---|---|
| I | 0.0000 | 0.0000 | 0.283 | 4.18 (9) |
| IT | −0.1714 (3) | −0.0857 (1) | −0.2855 (5) | 9.0 (1) |
| IB | 0.2158 (2) | 0.1079 (1) | 0.0153 (6) | 12.3 (2) |
| Mo | −0.0969 (2) | −0.0485 (1) | 0.0000 | 4.73 (9) |
| O | −0.224 (2) | −0.112 (1) | 0.130 (5) | 19 (3) |
| C1 | −0.303 (4) | −0.194 (4) | 0.072 (7) | 10 (2)* |
| C2 | −0.376 (3) | −0.224 (4) | 0.19 (1) | 12 (3)* |
| C4 | −0.250 (4) | −0.085 (4) | 0.274 (6) | 9 (2)* |
| C3 | −0.347 (5) | −0.142 (6) | 0.30 (1) | 21 (7)* |

[a] Starred values indicate atoms refined isotropically. Anisotropically refined atoms are given in the form of the equivalent isotropic displacement parameter defined as $^4/_3[a^2B_{11} + b^2B_{22} + c^2B_{33} + ab(\cos\gamma)B_{12} + ac(\cos\beta)B_{13} + bc(\cos\alpha)B_{23}]$.

**Table VII.** Positional Parameters and Their Estimated Standard Deviations for $MoI_3(EtCN)_3$[a]

| atom | x | y | z | B, Å² |
|---|---|---|---|---|
| I1 | −0.0763 (2) | 0.0452 (1) | 0.3102 (1) | 6.87 (5) |
| I2 | 0.3307 (2) | 0.2934 (1) | 0.3339 (2) | 7.21 (5) |
| I3 | −0.0351 (2) | 0.3361 (1) | 0.2332 (2) | 7.75 (5) |
| Mo | 0.1182 (2) | 0.1785 (1) | 0.3180 (2) | 4.47 (4) |
| N1 | 0.108 (2) | 0.221 (1) | 0.472 (1) | 5.9 (5) |
| N2 | 0.135 (1) | 0.124 (1) | 0.168 (1) | 4.4 (4) |
| N3 | 0.234 (2) | 0.055 (1) | 0.391 (2) | 6.2 (5) |
| C1 | 0.112 (2) | 0.237 (1) | 0.560 (2) | 6.2 (7) |
| C2 | 0.149 (2) | 0.090 (2) | 0.091 (2) | 5.5 (6) |
| C3 | 0.291 (2) | −0.007 (2) | 0.440 (2) | 7.6 (7) |
| C4 | 0.108 (2) | 0.262 (2) | 0.672 (1) | 7.2 (6) |
| C5 | 0.154 (2) | 0.041 (2) | −0.011 (2) | 7.6 (7) |
| C6 | 0.376 (3) | −0.088 (2) | 0.506 (2) | 8.3 (8) |
| C7 | 0.054 (3) | 0.354 (2) | 0.684 (2) | 8.1 (8) |
| C8 | 0.286 (3) | 0.037 (3) | −0.021 (2) | 12 (1) |
| C9 | 0.284 (3) | −0.178 (2) | 0.506 (2) | 9.4 (9) |

[a] Anisotropically refined atoms are given in the form of the equivalent isotropic displacement parameter defined as $^4/_3[a^2B_{11} + b^2B_{22} + c^2B_{33} + ab(\cos\gamma)B_{12} + ac(\cos\beta)B_{13} + bc(\cos\alpha)B_{23}]$.

dentate ligand). Three of these have been prepared and structurally characterized, with L = THF, MeCN, and PhCN, the former in two different crystalline forms. Since these compounds were always obtained as minor products of reactions involving molybdenum(II) and molybdenum(III) compounds, we shall first describe and discuss the chemical processes taking place and then give a description of the trinuclear clusters.

**(a) Decarbonylation Reactions.** When a THF solution of $MoI_2(CO)_3(THF)_2$ is warmed to the reflux temperature, a black solid is slowly formed. This material appears to be a mixture of two or more products, but its major component seems to be an oligomeric THF adduct of $MoI_2$, compound **1** (eq 1), according

$$MoI_2(CO)_3(THF)_2 \xrightarrow[-CO]{THF/\Delta} \underset{\mathbf{1}}{\{MoI_2(THF)_n\}_x} \quad (1)$$

to the following evidence: (i) it does not contain CO (IR analysis); (ii) analytical results are in accord with the formulation "$Mo_4I_8(THF)_3$"; (iii) this material reacts with nitriles and with $PMe_3$ to afford $Mo_2I_4L_4$ dimers (vide infra); (iv) it is known[13] that when the decarbonylation reaction is performed in the presence of monodentate (L) or bidentate (L–L) phosphine ligands, the compounds $Mo_2I_4L_4$ and $Mo_2I_4(L–L)_2$ are formed.

The $MoI_2(CO)_3(THF)_2$ starting material has been obtained in situ from $Mo_2I_4(CO)_8$.[14] It can also be obtained, however, by dissolving $[MoI(CO)_3(\eta^6\text{-arene})][Mo_2I_5(CO)_6]$, i.e., the product of $I_2$ oxidation of $Mo(CO)_3(\eta^6\text{-arene})$, in THF.[20]

The oligomeric nature of the product is in line with its insolubility in THF and in other solvents that are devoid of coordinating properties. The compound is always more or less contaminated by molybdenum(III) compounds. This is shown by the subsequent reactions of compound **1** (vide infra) and is rationalized on the basis of the known disproportionation of $MoX_2(CO)_3L_2$ compounds to $Mo(CO)_nL_{6-n}$ and $MoX_3L_3$ when L is a hard-donor ligand.[13b,21] The mother liquor of compound **1** shows an IR stretching vibration attributable to $Mo(CO)_6$, therefore suggesting the stoichiometry shown in eq 2 for the disproportionation reaction.

$$3MoI_2(CO)_3(THF)_2 \xrightarrow{THF} Mo(CO)_6 + 2MoI_3(THF)_3 + 3CO \quad (2)$$

This is a slow reaction at room temperature, but it will certainly be accelerated at the reflux temperature, and the Mo(III) product, which is only sparingly soluble in THF,[18] will contaminate compound **1**. The purification of compound **1** from the byproduct(s) is rendered difficult by the insolubility of the compounds and by their reactivity toward donor solvents. Magnetic susceptibility measurements were carried out on several samples of compound **1** coming from different runs of the preparation reaction and variable values for $\chi_g$ in the range (0.38–1.68) × $10^{-6}$ cgsu were obtained. Assuming that the pure compound **1** is diamagnetic (as suggested by its chemical behavior), this corresponds to the presence of 7–20% $MoI_3(THF)_3$ in various samples of the isolated product.

Similar IR spectroscopic and magnetic properties were observed for the product isolated from the thermal reaction of $Mo(CO)_3(THF)_3$ and $I_2$ in equimolar amounts (eq 3).

$$Mo(CO)_3(THF)_3 + I_2 \xrightarrow[-CO]{THF/\Delta} \{MoI_2(THF)_n\}_x \quad (3)$$

$Mo(CO)_3(THF)_3$ can be obtained in situ from the easily available $Mo(CO)_3(\eta^6\text{-arene})$ (e.g. arene = $C_6H_5CH_3$)[22] compounds.

A plausible formulation for the structure of compound **1**, based on the elemental analysis, is shown in I, but others with more

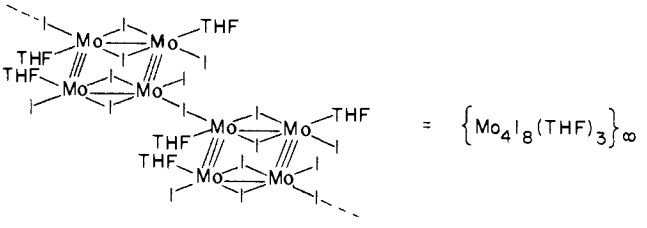


I

extended networks and a lower content of THF cannot be excluded, since the presence of the $MoI_3(THF)_3$ impurity in the analyzed sample may result in artificially higher C and H percentages, and there is, moreover, the possibility that interstitial THF molecules are trapped in the product. In any case, a rectangular array of molybdenum atoms is likely to be the building block of the structure of compound **1**. In fact, tetranuclear compounds of the type $Mo_4X_8L_4$ are known to be obtained[23] from the condensation reaction of the quadruply metal–metal bonded dimers $Mo_2X_4L_4$ (we remind the reader that the decarbonylation of $MoI_2(CO)_3L_2$ to $Mo_2I_4L_4$ has been established[13]), and they regenerate the $Mo_2X_4L_4$ dimers upon treatment with excess ligand L.[23] We hypothesize, therefore, that the decarbonylation of $MoI_2(CO)_3(THF)_2$ leads to $Mo_2I_4(THF)_4$ but this, being presumably unstable, condenses further to the oligonuclear structure of compound **1**.

From the mother liquor of compound **1**, obtained either from $Mo_2I_4(CO)_8$ or from $Mo(CO)_3(\eta^6\text{-}C_6H_5CH_3)$ and $I_2$, small amounts of black crystals formed slowly at room temperature. X-ray analysis (vide infra) shows them to be of a trinuclear

(20) Barbati, A.; Calderazzo, F.; Poli, R.; Zanazzi, P. F. *J. Chem. Soc., Dalton Trans.* **1986**, 2569.

(21) (a) Westland, A. D.; Muriithi, N. *Inorg. Chem.* **1972**, *11*, 2971. (b) Westland, A. D.; Muriithi, N. *Inorg. Chem.* **1973**, *12*, 2356.

(22) Strohmeier, W. *Chem. Ber.* **1961**, *94*, 3337.

(23) Ryan, T. R.; McCarley, R. E. *Inorg. Chem.* **1982**, *21*, 2072.

**Table VIII.** Selected Bond Distances (Å) and Angles (deg) for $MoI_3(EtCN)_3$[a]

| atom 1 | atom 2 | distance | atom 1 | atom 2 | distance |
|---|---|---|---|---|---|
| I1 | Mo | 2.760 (3) | Mo | N3 | 2.15 (2) |
| I2 | Mo | 2.763 (3) | N1 | C1 | 1.15 (3) |
| I3 | Mo | 2.741 (2) | N2 | C2 | 1.14 (3) |
| Mo | N1 | 2.11 (2) | N3 | C3 | 1.13 (3) |
| Mo | N2 | 2.12 (2) | | | |

| atom 1 | atom 2 | atom 3 | angle | atom 1 | atom 2 | atom 3 | angle |
|---|---|---|---|---|---|---|---|
| I1 | Mo | I2 | 173.47 (9) | I3 | Mo | N1 | 90.8 (4) |
| I1 | Mo | I3 | 93.68 (8) | I3 | Mo | N2 | 94.0 (4) |
| I1 | Mo | N1 | 89.1 (5) | I3 | Mo | N3 | 177.1 (6) |
| I1 | Mo | N2 | 89.1 (4) | N1 | Mo | N2 | 175.0 (6) |
| I1 | Mo | N3 | 85.0 (5) | N1 | Mo | N3 | 86.6 (7) |
| I2 | Mo | I3 | 92.84 (8) | N2 | Mo | N3 | 88.6 (7) |
| I2 | Mo | N1 | 91.3 (5) | Mo | N1 | C1 | 173 (2) |
| I2 | Mo | N2 | 90.0 (4) | Mo | N2 | C2 | 176 (2) |
| I2 | Mo | N3 | 88.6 (5) | Mo | N3 | C3 | 172 (2) |

[a] Numbers in parentheses are estimated standard deviations in the least significant digits.

**Table IX.** Positional Parameters and Their Estimated Standard Deviations for $Mo_2I_4(PhCN)_4$[a]

| atom | x | y | z | B, Å² |
|---|---|---|---|---|
| Mo | 0.0906 (1) | 0.1067 (1) | 0.8653 (2) | 4.86 (8) |
| I1 | 0.0105 (1) | 0.12278 (8) | 0.7543 (2) | 6.20 (7) |
| I2 | 0.1128 (1) | 0.05816 (9) | 0.9737 (2) | 6.96 (8) |
| N1 | 0.126 (1) | 0.0697 (8) | 0.784 (2) | 5.3 (7)* |
| N2 | 0.039 (1) | 0.1290 (9) | 0.952 (2) | 7.5 (9)* |
| C1 | 0.151 (1) | 0.049 (1) | 0.746 (2) | 5.2 (9)* |
| C2 | 0.006 (1) | 0.1398 (9) | 0.984 (2) | 4.5 (8)* |
| C10 | 0.178 (1) | 0.0278 (9) | 0.699 (2) | 3.9 (8)* |
| C11 | 0.211 (1) | 0.0392 (9) | 0.634 (2) | 4.7 (8)* |
| C12 | 0.240 (2) | 0.016 (1) | 0.586 (2) | 7 (1)* |
| C13 | 0.235 (2) | −0.018 (1) | 0.610 (2) | 7 (1)* |
| C14 | 0.203 (2) | −0.030 (1) | 0.666 (2) | 6 (1)* |
| C15 | 0.172 (1) | −0.005 (1) | 0.718 (2) | 7 (1)* |
| C20 | −0.034 (1) | 0.157 (1) | 1.049 (2) | 5.4 (9)* |
| C21 | −0.005 (2) | 0.173 (1) | 1.109 (2) | 7 (1)* |
| C22 | −0.047 (2) | 0.189 (1) | 1.163 (3) | 10 (1)* |
| C23 | −0.107 (1) | 0.188 (1) | 1.154 (2) | 5.1 (9)* |
| C24 | −0.131 (2) | 0.171 (1) | 1.101 (2) | 6 (1)* |
| C25 | −0.155 (1) | 0.153 (1) | 0.704 (2) | 6 (1)* |

[a] Starred values indicate atoms refined isotropically. Anisotropically refined atoms are given in the form of the equivalent isotropic displacement parameter defined as $^4/_3[a^2B_{11} + b^2B_{22} + c^2B_{33} + ab(\cos\gamma)B_{12} + ac(\cos\beta)B_{13} + bc(\cos\alpha)B_{23}]$.

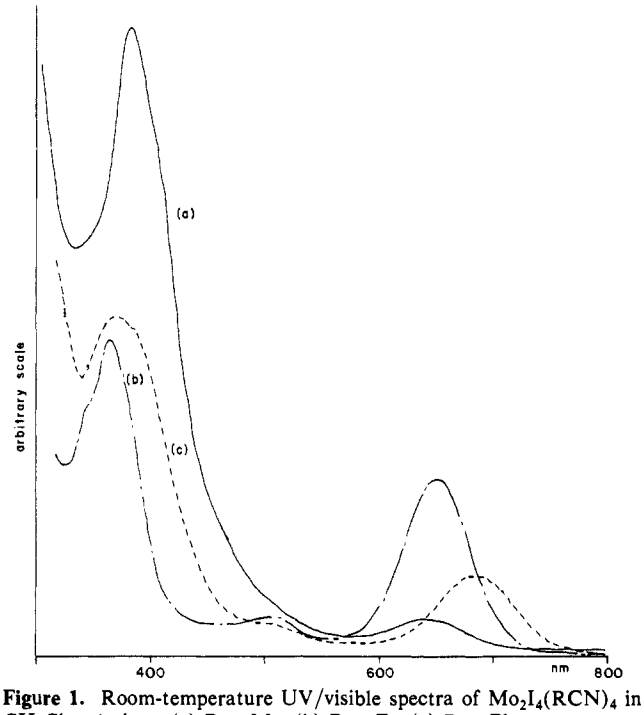


**Figure 1.** Room-temperature UV/visible spectra of $Mo_2I_4(RCN)_4$ in $CH_2Cl_2$ solution: (a) R = Me; (b) R = Et; (c) R = Ph.

compound, $Mo_3HI_7(THF)_3 \cdot THF$ (**2**). The physico–chemical, structural, and bonding properties of compound **2**, are discussed in section (c), together with those of other similar trinuclear clusters.

The thermal decarbonylation of $MoI_2(CO)_3(RCN)_2$ (R = Me, Et), obtained in situ from $Mo_2I_4(CO)_8$,[14] in the corresponding nitrile, affords green solutions and minor amounts of a brown insoluble solid. These green solutions are identical with those obtained by the room-temperature interaction of compound **1** with the corresponding nitrile. We believe they contain the compounds $Mo_2I_4(RCN)_4$ (R = Me, Et). Contrary to the decarbonylation reaction carried out in THF, therefore, those carried out in acetonitrile and propionitrile produce quadruply bonded dimers that are stable *when dissolved in the ligand itself as solvent*. These products could not be isolated from the solutions, however, as evaporation to dryness led to the formation of brown materials, which might be formulated similarly to compound **1** (see eq 4). These materials furnish solutions of the corresponding dimer when redissolved in the nitrile.

The formulation of the products of the decarbonylation reactions as quadruply bonded dimers is supported by their UV/visible

**Table X.** Bond Distances (Å) and Angles (deg) for $Mo_2I_4(PhCN)_4$[a]

| atom 1 | atom 2 | distance | atom 1 | atom 2 | distance |
|---|---|---|---|---|---|
| Mo | Mo′ | 2.144 (5) | Mo | N2 | 2.10 (3) |
| Mo | I1 | 2.735 (4) | N1 | C1 | 1.19 (5) |
| Mo | I2 | 2.731 (5) | N2 | C2 | 1.03 (5) |
| Mo | N1 | 2.19 (3) | | | |

| atom 1 | atom 2 | atom 3 | angle | atom 1 | atom 2 | atom 3 | angle |
|---|---|---|---|---|---|---|---|
| Mo′ | Mo | I1 | 109.7 (2) | I1 | Mo | N2 | 91.6 (9) |
| Mo′ | Mo | I2 | 109.7 (2) | I2 | Mo | N1 | 84.6 (8) |
| Mo′ | Mo | N1 | 100.2 (7) | I2 | Mo | N2 | 85 (1) |
| Mo′ | Mo | N2 | 97.4 (9) | N1 | Mo | N2 | 162 (1) |
| I1 | Mo | I2 | 140.6 (2) | Mo | N1 | C1 | 172 (3) |
| I1 | Mo | N1 | 87.3 (7) | Mo | N2 | C2 | 166 (3) |

[a] Numbers in parentheses are estimated standard deviations in the least significant digits.

$$MoI_2(CO)_3(RCN)_2 \xrightarrow{RCN/\Delta} Mo_2I_4(RCN)_4 \underset{RCN}{\overset{\text{evaporation}}{\rightleftharpoons}} \{MoI_2(RCN)_n\}_x \quad (4)$$

spectra (see Figure 1). The $\delta \rightarrow \delta^*$ band (band I) is observed at 643 nm for $Mo_2I_4(MeCN)_4$ and at 645 nm for $Mo_2I_4(EtCN)_4$ (as compared, for example, with 631 nm for $Mo_2I_4(PMe_3)_4$[13a,24,25]). These spectra also show the characteristic band at the borderline between visible and UV regions (band II), which has recently been attributed to a charge-transfer transition,[25] at 392 nm (R = Me) and 360 nm (R = Et), to be compared with 394 nm for $Mo_2I_4(PMe_3)_4$.[13a,24,25] The presence of $Mo_2I_4(RCN)_4$ in these solutions is also supported by the formation of $Mo_2I_4(PMe_3)_4$ upon treatment with $PMe_3$ and by the isolation and structural characterization of $Mo_2I_4(PhCN)_4$, obtained by ligand exchange (vide infra).

The byproduct of the thermal reaction in acetonitrile has been isolated and characterized: it is the trimer $Mo_3HI_7(MeCN)_3 \cdot MeCN$ (**3**), which is related to compound **2**.

**(b) Reactivity of Compound 1.** When compound **1** is treated with nitriles, a reaction occurs with production of solutions of the dimers $Mo_2I_4(RCN)_4$ (R = Me, Et, Ph); see eq 5.

$$\{MoI_2(THF)_n\}_x \xrightarrow{RCN} Mo_2I_4(RCN)_4 \quad (5)$$

R = Me, Et, Ph

Small amounts of red insoluble material are also obtained when reaction 5 is carried out with each nitrile ligand. These red substances are believed to be derived from the molybdenum(III) impurities that we know to be present in compound **1**, as discussed above. The isolated byproduct of the reaction in propionitrile is a mononuclear compound, i.e. $MoI_3(EtCN)_3$ (**4**). As expected, this compound has two CN stretching vibrations, at 2278 and 2270 $cm^{-1}$.

From the benzonitrile reaction, a few crystals of compound $Mo_3HI_7(PhCN)_3 \cdot C_6H_5CH_3$ (**5**) were obtained.

Only for R = Ph was it possible to isolate the product of eq 5 in the solid state (compound **6**), whereas for R = Me and Et oligonuclear compounds were obtained as discussed above; see eq 4. This was accomplished via ligand exchange from $Mo_2I_4(RCN)_4$ (R = Me, Et; eq 6), the intermediate being in turn obtained by

$$Mo_2I_4(RCN)_4 \xrightarrow{L} Mo_2I_4L_4 \quad (6)$$

R = Me, Et; L = PhCN, $PMe_3$

the thermal reaction depicted in eq 4. This route afforded a product that is less contaminated by compound **5** than the one obtained by the direct interaction of compound **1** with PhCN (eq 5). The UV/visible spectra of $CH_2Cl_2$ solutions of the three $Mo_2I_4(RCN)_4$ (R = Me, Et, Ph) dimers are compared in Figure 1. A substantial red shift of band I ($\delta \rightarrow \delta^*$) is observed on going from R = Me and Et to R = Ph, which may be caused by a $\pi$ interaction between the aromatic nitrile and the metal d orbitals.

The higher stability of $Mo_2I_4(PhCN)_4$ toward loss of nitrile, as compared to its lighter nitrile analogues, might be associated with a stronger bonding to the aromatic nitrile, a feature that is not inconsistent with the results of the electronic spectroscopy, and perhaps also with the lower volatility of the ligand. However, even compound **6** also has a tendency to lose the nitrile ligand. In fact, when a sample of the isolated solid is dissolved in neat $CH_2Cl_2$, the visible absorptions shown in Figure 1 were not observed for the resulting solution. These were partially regained upon further treatment with excess benzonitrile. For this reason, the spectra reported in Figure 1 could not be obtained on an absolute scale.

To the best of our knowledge, compound **6** is the first $Mo_2X_4L_4$ compound containing nitrile ligands for which a crystal structure is reported (vide infra). Other known nitrile compounds of quadruply bonded molybdenum dimers, though with a different halide ligand, are $Mo_2Cl_4(RCN)_4$ (R = Me, Ph).[26]

A ligand-exchange reaction (eq 6) also takes place when an interaction with $PMe_3$ is carried out, with production of the known[13a,24,25] $Mo_2I_4(PMe_3)_4$. When, on the other hand, compound **1** is dissolved in RCN (R = Et) and then treated with $I^-$, the known[10] $[Mo_4I_{11}]^{2-}$ anion is obtained in good yields and can be isolated as its $AsPh_4^+$ salt (eq 7).

$$Mo_2I_4(EtCN)_4 \xrightarrow{I^-} [Mo_4I_{11}]^{2-} \quad (7)$$

The identity of $[AsPh_4]_2[Mo_4I_{11}]$ is established by elemental analysis. In addition, an X-ray analysis has been performed.[27] A geometry for the $[Mo_4I_{11}]^{2-}$ ion corresponding to that reported for the $n$-$Bu_4N^+$ salt[10] has been found, but the structure could not be fully refined because of twinning problems, and we do not, therefore, discuss it in detail.

It is likely that the tetranuclear cluster is formed by condensation of two dinuclear units, followed by a one-electron oxidation to the +2.25 average oxidation state. The oxidizing agent is probably a molybdenum(III) species, which is known to be present as an impurity in compound **1**.

We draw attention to the fact that the $[Mo_4I_{11}]^{2-}$ cluster was first obtained[10] by thermal decarbonylation of $[MoI_3(CO)_4]^-$. Taking into account that the latter can be obtained by interacting $Mo_2I_4(CO)_8$ with $I^-$,[14] this amounts to saying that the original preparation and our preparation of the $[Mo_4I_{11}]^{2-}$ cluster differ merely in the order of operations when starting from $Mo_2I_4(CO)_8$: interaction with $I^-$, followed by thermal decarbonylation, in the original synthesis[10] and decarbonylation followed by interaction with $I^-$ in the one that we report here.

Once it had been established that compound **1** can be used as a convenient starting material for the preparation of $Mo_2I_4L_4$ compounds under mild conditions, we wondered whether we could prepare such a compound with the ligand $PPh_3$. No $M_2X_4L_4$ compound with four $PPh_3$ ligands is known to date, and steric factors militate against its possible formation. Interaction of compound **1** with $PPh_3$ did take place, but the only crystalline material that we could obtain is $Mo_3HI_7(THF)_3$ (**7**), in a crystalline form different from that of its THF adduct (compound **2**).

**(c) $Mo_3HI_7L_3$ Clusters.** The compounds $Mo_3HI_7(THF)_3 \cdot THF$ (**2**), $Mo_3HI_7(MeCN)_3 \cdot MeCN$ (**3**), $Mo_3HI_7(PhCN)_3 \cdot C_6H_5CH_3$ (**5**), and $Mo_3HI_7(THF)_3$ (**7**) were characterized structurally by X-ray techniques. All these materials were adventitiously obtained as minor products of the reactions discussed in the previous sections. The IR spectrum (Nujol mull) of compound **2** (4000–250 $cm^{-1}$) shows only bands attributable to the THF molecules and is similar but not identical with that of compound **1**. Compound **3** exhibits two stretching vibrations for the coordinated acetonitrile ligands at 2307 and 2277 $cm^{-1}$, in agreement with expectation for the $C_{3v}$ symmetry of the molecule. An additional weak band at 2248 $cm^{-1}$ might be attributed to the free acetonitrile molecule (a mixture of MeCN and Nujol shows the CN stretching vibration at 2253 $cm^{-1}$). In compound **5**, on the other hand, the CN stretching vibrations are seen as a broader band at 2245 $cm^{-1}$ with a shoulder at 2230 $cm^{-1}$, and the entire spectrum is practically identical with that of compound **6**. Free benzonitrile (dissolved in Nujol) absorbs at 2233 $cm^{-1}$.

A general view of the $Mo_3$ coordination sphere in the $Mo_3HI_7L_3$ clusters is shown in Figure 2. The trimers in the solvated structures (compounds **2**, **3**, and **5**) have crystallographically imposed mirror planes passing through the Mo(1), I(1), I(22), and O(1) (for THF) or N(1) (for MeCN and PhCN) atoms. A top view of the molecule is shown in Figure 3 for compound **2**, Figure 4 for compound **3**, and Figure 5 for compound **5**. The interstitial solvent molecule lies on a crystallographic twofold axis

(24) Cotton, F. A.; Poli, R. *Inorg. Chem.* **1987**, *26*, 3652.
(25) Hopkins, M. D.; Schaefer, W. P.; Bronikowski, M. J.; Woodruff, W. H.; Miskowski, V. M.; Dallinger, R. F.; Gray, H. B. *J. Am. Chem. Soc.* **1987**, *109*, 408.
(26) San Filippo, J., Jr.; Sniadoch, H. J.; Grayson, R. L. *Inorg. Chem.* **1974**, *13*, 2121.
(27) Crystal data for $[AsPh_4]_2[Mo_4I_{11}]$: monoclinic; space group $P2_1/m$; $a$ = 12.242 (9), $b$ = 24.519 (9), $c$ = 11.200 (7) Å; $\beta$ = 103.72 (4)°; $V$ = 3266 (6) Å$^3$; $Z$ = 2; $d_{calcd}$ = 2.589 g·cm$^{-3}$.

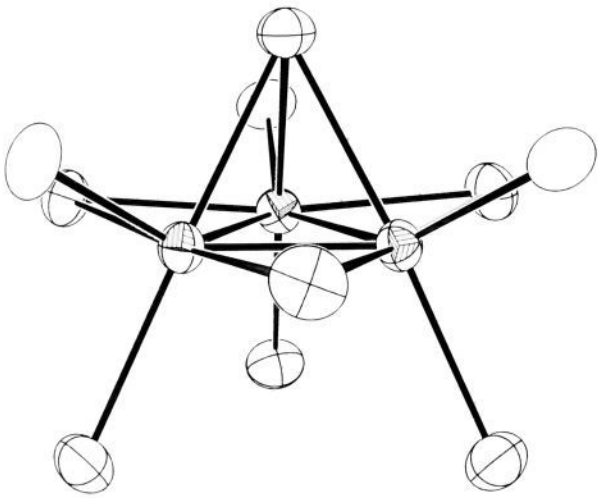

**Figure 2.** View of the core of the $Mo_3HI_7L_3$ compounds.

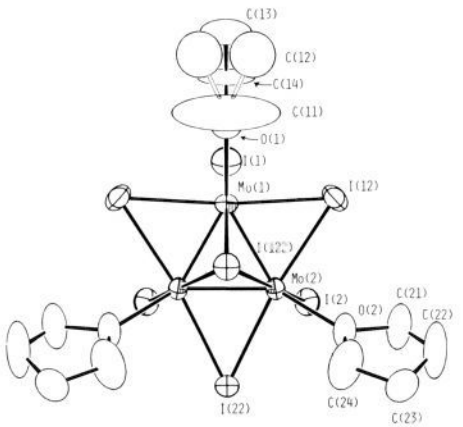


**Figure 3.** Top view of the trinuclear cluster in compound **2**.

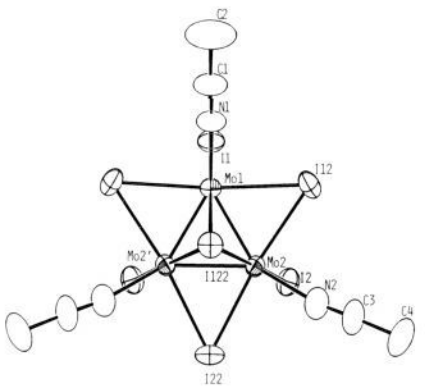


**Figure 4.** Top view of the trinuclear cluster in compound **3**.

for the isostructural compounds **2** and **3** and on an inversion center for compound **5**. The unsolvated trimer, $Mo_3HI_7(THF)_3$ (**7**), has the same molecular geometry (Figure 6), but the crystallographically imposed symmetry is higher, i.e. $C_{3v}$. It is interesting to note that the coordinated THF molecules are disordered in both compounds **2** and **7** wherever they are found sitting on a crystallographic mirror plane. For compound **2** we tried to refine the structure without the crystallographic mirror plane (by using the noncentrosymmetric space group $Pca2_1$), but this led to severe correlations, from which we conclude that the centrosymmetric space group is the correct choice. For compound **7** the situation is even clearer, as removal of the mirror plane would result in a change of Laue class.

As stated in the introduction, these trinuclear clusters can be viewed as fragments of the $[Mo_6I_8]^{4+}$ cluster core found in the

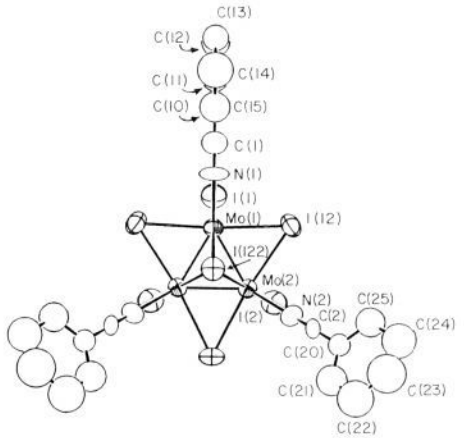


**Figure 5.** Top view of the trinuclear cluster in compound **5**.

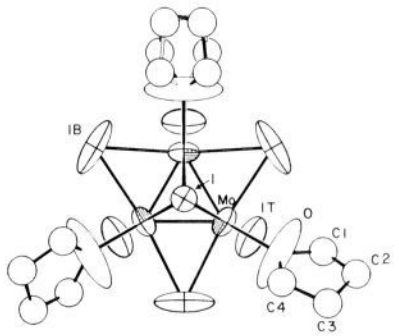


**Figure 6.** Top view of compound **7**. The statistical disorder is shown on only one of the three equivalent THF molecules.

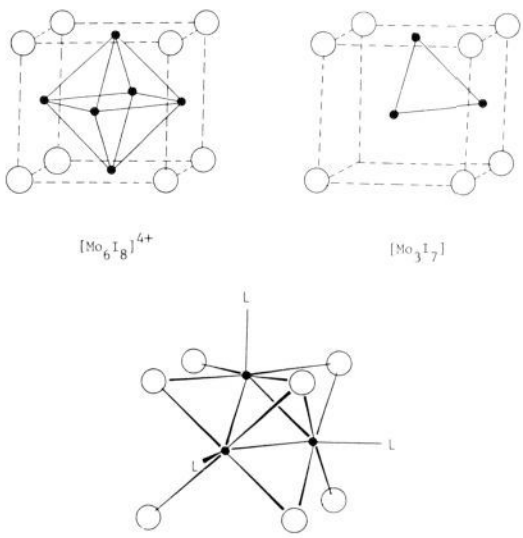


**Figure 7.** Representation of the structures of the $[Mo_6I_8]^{4+}$ and $[Mo_3I_7]^+$ cluster cores showing the relationship between the two units.

structure of $\alpha$-$MoI_2$.[2] The relationship between the two cores is illustrated in Figure 7. The $Mo_3I_7$ structure can formally be obtained from the $Mo_6I_8$ structure by removing one $Mo_3$ triangle with its capping iodide ion. Three iodide ions then become doubly bridging while another three become terminal. The three L groups in $Mo_3HI_7L_3$ occupy terminal positions corresponding to the iodide ions that bridge different $[Mo_6I_8]^{4+}$ units in $\alpha$-$MoI_2$.[2] The hydrogen atom could not be located during the refinement of the structures, but the most likely position is a triply bridging one, opposite to that occupied by the triply bridging iodide ligand. This is also consistent with the results of an $^1H$ NMR study on com-

pound **5** (vide infra). The placement of the hydrogen atom in such a triply bridging position completes an octahedral geometry of the ligands around each molybdenum atom.

The Mo–Mo distances (ranging from 2.487 to 2.541 Å) are indicative of strong bonding interactions, especially when the presence of the bulky bridging iodide ligands is taken into account. The value found for $\alpha$-$MoI_2$ (where the metal–metal interaction has been described as being of bond order 1)[8] is 2.672 Å.[2] It is evident from the views in Figures 3–6 that the $Mo_3$ triangle has shrunk toward the center with respect to the triangle determined by the three doubly bridging iodide ions, with $I_{br}$–Mo–$I_{br}$ angles averaging 171.4 [7]° for **2**, 170.8 [5]° for **3**, 170.9 [4]° for **5**, and 171.4 (2)° for **7** (vs 177.0° in $\alpha$-$MoI_2$[28]). Other good indications of strong metal–metal bonding interactions are the small Mo–$I_{br}$–Mo angles (average 53.37 [11]° for **2**, 54.08 [24]° for **3**, 54.00 [7]° for **5**, and 53.2 (1)° for **7**) and Mo–$I_{cap}$–Mo angles (average 52.63 [2]° for **2**, 54.11 [5]° for **3**, 53.22 [10]° for **5**, and 52.25 (8)° for **7**). These are to be compared with 57.6° for $\alpha$-$MoI_2$.[28] The values indicate that the bond strength increases in the order MeCN < PhCN < THF, which parallels the decrease of Lewis basicity of the ligands. The molecular orbital calculations (discussed later) give support to the crystallographic evidence for strong metal–metal bonds.

The Mo–I bond lengths increase, as expected, in the sequence terminal (2.689 [4] Å for **2**, 2.709 [5] Å for **3**, 2.673 [4] Å for **5**, 2.692 (4) Å for **7**) < bridging (2.793 [6] Å for **2**, 2.794 [10] Å for **3**, 2.782 [9] Å for **5**, 2.777 (3) Å for **7**) < capping (2.830 [3] Å for **2**, 2.793 [3] Å for **3**, 2.819 [12] Å for **5**, 2.824 (2) Å for **7**) with the notable exception of the Mo–$I_{cap}$ distance for **3**, which is the same as the Mo–$I_{br}$ distance in the same compound, within the experimental error.

Structurally, $Mo_3HI_7L_3$ (L = monodentate neutral ligand) represents a new type of triangular cluster for group 6 metals. Prototypes of other types of triangular geometries are the bicapped $M_3(\mu_3\text{-}O)_2(\mu\text{-}O_2CR)_6L_3$ (M = Mo, W)[29,30] [coordination number (CN) = 9], the monocapped $[Mo_3(\mu_3\text{-}O)(\mu\text{-}O)_3(C_2O_4)_3(H_2O)_3]^{2-}$ (CN = 8),[31] the monocapped $[W_3(\mu_3\text{-}O)(\mu\text{-}O)_3(O_2CCH_3)_6(H_2O)_3]^{2+}$ (CN = 8),[32] and the bicapped $[Mo_3(\mu_3\text{-}O)(\mu_3\text{-}OR)(\mu\text{-}OR)_3(OR)_6]$ (CN = 8).[33] A recent survey on trinuclear molybdenum clusters is available.[34] The coordination number in $Mo_3HI_7L_3$ is 8 (each molybdenum atom is surrounded by four iodide ions, the hydride, one L ligand, and the other two molybdenum atoms), and the geometry is formally similar to that of the $[Mo_3O(OR)_{10}]$ compounds mentioned above,[33] but the latter are more symmetric, and the metal–metal interaction is less because of the higher average oxidation state. From the electronic point of view, our $Mo_3HI_7L_3$ clusters can be considered to be more similar to $Re_3Cl_9L_3$,[35] both classes of compounds having a higher number of electrons for cluster bonding and strong metal–metal interactions. A relationship between the $Re_3Cl_9L_3$ clusters and our $Mo_3HI_7L_3$ molecules can be envisioned by fusing three axial chloride ions of the former into a capping ligand and providing a hydrogen atom to fill in the coordination site in the opposite capping position.

The most crucial problem encountered in this study has been the assignment of the oxidation state to the trinuclear clusters. The presence of the hydrogen atom was not initially realized, since it is not evident from the X-ray data. The hypothetical $Mo_3I_7L_3$ structure would have 11 electrons available for cluster bonding, and we noticed that most of the other low-valent discrete clusters

**Scheme II**[a]

$$Mo_2I_4I_4 + MoI_3L_3 \longrightarrow \text{"}Mo_3I_7L_3\text{"} + 3L \xrightarrow{\text{"active C–H"}} Mo_3HI_7L_3$$

[a] L = THF, RCN.

of molybdenum known to date have an odd number of electrons, e.g., 19 for $[Mo_5Cl_{13}]^{2-}$,[9] 15 for $[Mo_4I_{11}]^{2-}$,[10] and 15 for the two isomeric forms of $[Mo_4Cl_{12}]^{3-}$.[11] It seemed possible to push the analogy even further: all of the above-mentioned clusters, as well as the hypothetical $Mo_3I_7L_3$, have one electron less that the number calculated for a pure Mo(II) cluster; in other words, they all formally consist of $(n-1)$ Mo(II) ions plus 1 Mo(III) ion. We therefore made a considerable effort to find experimental evidence for (or against) the odd-electron formulation.

Compound **2** was found to be EPR silent down to liquid nitrogen temperature. Electronic structure calculations (discussed below) on the $C_{3v}$-idealized $Mo_3I_7(H_2O)_3$ model compound predicted that the HOMO would be an $a_1$ orbital, substantially metal based and slightly metal–metal bonding in character. Because of possible interactions between an unpaired electron in this orbital and the many quadrupolar nuclei, and/or the presence of low-lying excited states, we considered it possible that a still lower temperature might be necessary to produce an observable EPR signal. The radical anions $[Os_{10}X(CO)_{24}]^{\cdot-}$ (X = C, $H_4$)[36] may be cited as known examples of this possibility. It is not feasible to make measurements at lower temperatures with our equipment. However, we were able to prepare enough of compound **2** for a magnetic susceptibility study to be performed down to 5 K, in order to minimize the error caused by the diamagnetic contribution. A trace of paramagnetic impurity was observed, which followed the Curie–Weiss law in the whole range of temperatures studied; this corresponded to only about 2% of free spins in the trinuclear product. The molar diamagnetic correction was estimated to be $B = -320 \times 10^{-6}$ cgsu from the intercept of the $\chi$ vs $1/T$ plot. Compound **2** is therefore intrinsically diamagnetic, and the small paramagnetism is probably due to paramagnetic impurities deposited, or formed by aerial oxidation, on the surface of the crystals.

This finding turned our attention to the possibility of having an additional hydrogen atom in the structure. A tentative location for it could have been on the interstitial THF molecule, to form a $[H(THF)]^+$ cation. A similar situation has been reported for the compound $[H(THF)_2]^+[Nb_2Cl_3(CO)_8]^-$.[37] This idea was discarded once we obtained the crystal structures of the other trimers, particularly those of compound **5**, with interstitial toluene, and compound **7**, which does not contain interstitial solvent at all. The only other plausible location for a hydrogen atom is the capping position opposite to that occupied by the triply bridging iodide, as discussed earlier. Compounds **2** and **3** are unfortunately too insoluble in any unreactive solvent for NMR studies to be performed. Compound **5**, on the other hand, is slightly soluble in $CH_2Cl_2$, and a $^1H$ NMR spectrum could be recorded. This confirmed that the compound is diamagnetic but, more important, revealed a sharp peak at $\delta$ −10.31, assigned to the triply bridging hydride ion. The hydridic nature of the capping hydrogen atom, which this chemical shift value suggests, is supported by electronic structure calculations to be described presently.

Given the presence of the additional hydrogen atom, we asked ourselves where it comes from. Answering this question implies having an idea about the mechanism by which the trinuclear clusters are formed. Although we do not have any proof, we can advance a few suggestions. A possible source of the hydrogen atom is adventitious moisture, especially considering that the compounds were always obtained in trace amounts. The stoichiometry of the materials suggests a formal interaction between a "$Mo_3I_6$" cluster core of molybdenum(II) and HI. The former may possibly be assembled by the interaction of the dimer $Mo_2I_4L_4$ (which is present in solution for L = RCN or can be formed as a transient

(28) Value calculated from the atomic coordinates in ref 2.
(29) Bino, A.; Cotton, F. A.; Dori, Z.; Koch, S.; Küppers, H.; Millar, M.; Sekutowski, J. C. *Inorg. Chem.* **1978**, *17*, 3245.
(30) Ardon, M.; Bino, A.; Cotton, F. A.; Dori, Z.; Kaftory, M.; Reisner, G. *Inorg. Chem.* **1982**, *21*, 1912.
(31) Bino, A.; Cotton, F. A.; Dori, Z. *J. Am. Chem. Soc.* **1978**, *100*, 5252.
(32) Ardon, M.; Cotton, F. A.; Dori, Z.; Fang, A.; Kapon, M.; Reisner, G. M.; Shaia, M. *J. Am. Chem. Soc.* **1982**, *104*, 5394.
(33) Chisholm, M. H.; Folting, K.; Huffman, J. C.; Kirkpatrick, C. C. *J. Am. Chem. Soc.* **1981**, *103*, 5967.
(34) Cotton, F. A. *Polyhedron* **1986**, *5*, 3.
(35) Bertrand, J. A.; Cotton, F. A.; Dollase, W. A. *J. Am. Chem. Soc.* **1963**, *85*, 1349.
(36) Drake, S. R.; Johnson, B. F. G.; Lewis, J.; McQueen, R. C. S. *J. Chem. Soc., Dalton Trans.* **1987**, 1051.
(37) Calderazzo, F.; Castellani, M.; Pampaloni, G.; Zanazzi, P. F. *J. Chem. Soc., Dalton Trans.* **1985**, 1989.

Chart I

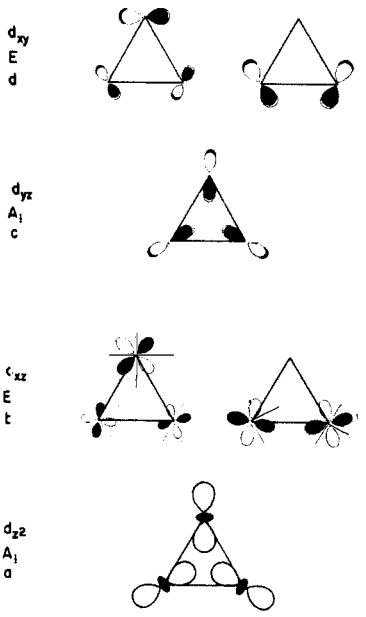


species from compound **1** for L = THF) with a mononuclear species of molybdenum(II). The origin of HI would remain to be established. Another, more attractive, possibility is that the trinuclear unit is formed from $Mo_2I_4L_4$ and a mononuclear molybdenum(III) compound (which is also present in solution in smaller concentrations) followed by a redox reaction that may involve a C–H bond of the solvent, as shown in Scheme II. This would imply that organic products coming from the oxidative coupling of the solvent should also be formed. This has not been verified, and we deferred this aspect of the study, as well as the search for a high-yield synthesis of these trinuclear clusters, to a future time.

A Fenske–Hall calculation[19a] has been carried out on the model compounds $Mo_3I_7L_3$ and $Mo_3HI_7L_3$ (L = $H_2O$ and HCN). The objectives of these calculations were (i) to find support for the observed strong metal–metal interactions and (ii) to identify the nature and interactions of the capping hydrogen atom. Simple geometric considerations would suggest that we should find the interactions illustrated in Chart I for the $Mo_3(\mu\text{-}I)_3$ planar frame, listed in increasing energy order.

The $d_{x^2-y^2}$ orbitals are directed along the bonds with the bridging iodide ligands, and their energy is therefore raised. The introduction of the other ligands will produce several effects that are not easily predictable because of the particular arrangement of the metal coordination spheres. At the very least we would, however, expect that the introduction of the capping iodide ligand should raise the energy of the orbital labeled as c; this should be raised even further upon introduction of the hydrogen atom in the opposite capping position.

The results of the calculations are summarized in the MO diagram shown in Figure 8. A complete listing of the molecular orbital energies for each compound, also showing the atomic contribution of the different kinds of atoms, is included in the supplementary material. We shall discuss first the hypothetical clusters that lack the capping hydrogen atom. The interpretation of the results presents a few problems because of extensive mixing of the metal orbitals with the ligand system, which is caused by the particular geometry. In particular, the degenerate metal–metal bonding interaction due to the Mo $d_{xz}$ orbitals, i.e. that labeled as b in Chart I, is spread among several MOs, mainly the 23e (44% Mo, of which 66% $d_{xz}$) and 24e (33% Mo, of which 43% $d_{xz}$) molecular orbitals for $Mo_3I_7(H_2O)_3$ and the 24e (43% Mo, of which 66% $d_{xz}$) and 25e (36% Mo, of which 43% $d_{xz}$) molecular orbitals for $Mo_3I_7(HCN)_3$ (MOs labeled b in Figure 8). The other three metal–metal interactions illustrated in Chart I can be more easily identified. They are, for $Mo_3I_7(H_2O)_3$, $16a_1$ (80% Mo, of which 58% $d_{z^2}$) (a), 27e (68% Mo, of which 84% $d_{xy}$) (d), and

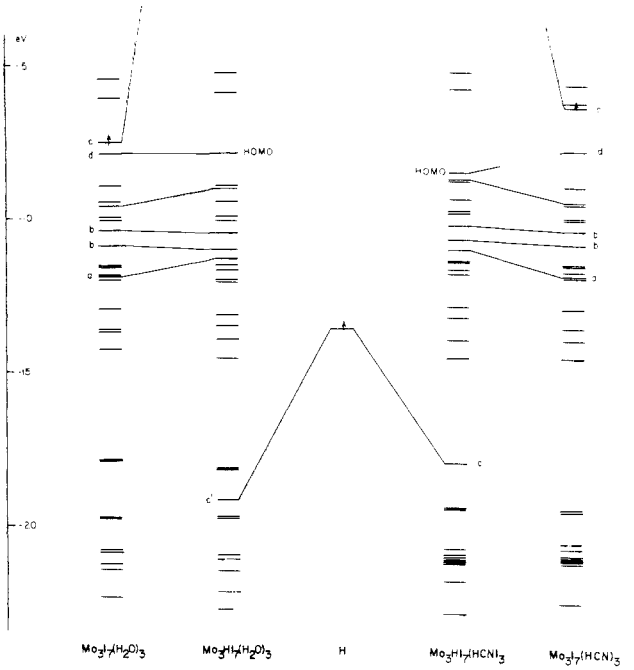


**Figure 8.** Molecular orbital diagram showing the interaction between $Mo_3I_7L_3$ and H (L = $H_2O$, HCN).

$20a_1$ (75% Mo, of which 58% $d_{yz}$) (c) and, for $Mo_3I_7(HCN)_3$, $17a_1$ (78% Mo, of which 59% $d_{z^2}$) (a), 28e (70% Mo, of which 82% $d_{xy}$) (d), and $21a_1$ (78% Mo, of which 51% $d_{yz}$) (c). As anticipated, the energy of the MO corresponding to interaction c is raised higher than that of interaction d (see Figure 8). All of the four interactions discussed (a–d) are of metal–metal bonding character. We therefore have, for each compound, 11 electrons to be used for cluster bonding and a formal metal–metal bond order of $^{11}/_{6}$.

The introduction of the hydrogen atom in the capping position has the effect illustrated in Figure 8: the main perturbation on the MO diagram is due to the interaction of the H 1s orbital with the molecular orbital labeled c. This is illustrated below:

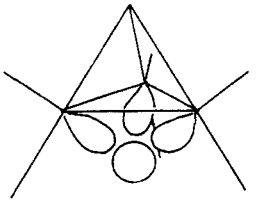

As a result, a new $a_1$ orbital with a relatively low energy is generated ($13a_1$ for $MoHI_7(H_2O)_3$, $15a_1$ for $Mo_3HI_7(HCN)_3$, both labeled c′ in Figure 8), to which the H 1s orbital contributes most (41% H, 13% Mo in the water adduct; 49% H, 18% Mo in the HCN adduct). It would therefore seem that the best description of the cluster–H interaction is that of a hydridic hydrogen donating its two electrons to a cluster molecular orbital of appropriate symmetry. This is in accord with the $^1H$ NMR results (vide supra). Most of the other MOs do not vary their energy much, including the metal–metal bonding MOs (a, b, and d). Therefore, the $Mo_3HI_7L_3$ (L = $H_2O$, HCN) molecules still enjoy strong metal–metal interactions, as is experimentally observed for the THF and nitrile adducts. There are now 10 electrons available for cluster bonding (under the assumption of a $Mo_3^{8+}$ core and a hydridic hydrogen), and they are all located in metal–metal bonding orbitals, for a formal bond order of ($^{10}/_{6}$) and an average oxidation state of $2^2/_3$.

To sum up, the Fenske–Hall MO calculations on the model compounds $Mo_3HI_7L_3$ (L = $H_2O$, HCN) support the presence of strong metal–metal interactions in the trinuclear compounds **2**, **3**, **5**, and **7** and suggest that these clusters be considered as mixed-valence compounds (having an $Mo_3^{8+}$ core), with 10 electrons used for cluster bonding and a hydride ($H^-$) capping ligand. The calculations also show that the hydride-capped clusters

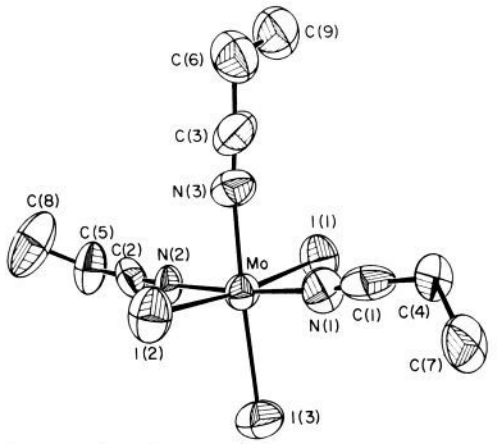


**Figure 9.** ORTEP view of compound **4**.

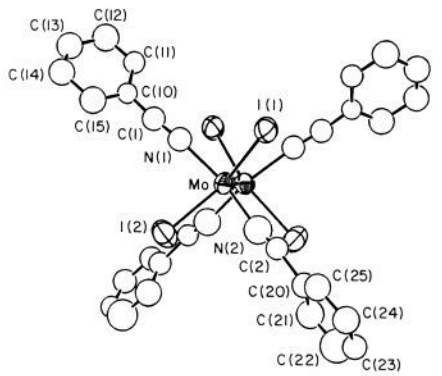


**Figure 10.** ORTEP view of compound **6**.

gain considerably in stability with respect to the hypothetical molecules that do not contain the $H^-$ cap.

**(d) Molecular Structures of Compounds 4 and 6. (i) $MoI_3(EtCN)_3$.** The geometry of the molecule (Figure 9) is octahedral with a meridional configuration. This is common to other six-coordinate compounds of +III metals of group 6 [e.g. $MoI_3(THF)_3$,[18] $MoCl_3(py)_3$,[38] $MoBr_3(4\text{-pic})_3$,[39] $CrCl_3(THF)_3$[40]] and of other groups [e.g., $MCl_3(THF)_3$ (M = Sc,[41] Ti,[42] V[40])]. The Mo–ligand distances (see Table VIII) show the expected trends according to the nature of the trans ligand, in agreement with the $I^- > EtCN$ trans influence. The Mo–I distances are similar to those of other Mo(III)–iodide complexes (e.g. 2.762 [6] Å in $MoI_3(PMe_2Ph)_2(POMe_2Ph)$,[13b] 2.786 [4] Å in $[MoI_4(PEt_2Ph)_2]^-$,[13b] 2.775 [25] Å in $MoI_3(THF)_3$,[18] 2.764 [9] Å for the terminal iodide ligands in $[PHMe_3][Mo_2I_7(PMe_3)_2]$[43]). The Mo–N distances in compound **4** are, on the average, shorter than the same distances in compounds **3**, **5**, and **6**, in agreement with the higher oxidation state of the former.

**(ii) $Mo_2I_4(PhCN)_4$.** The molecule (Figure 10) lies on a crystallographically imposed twofold axis, which is perpendicular to the molybdenum–molybdenum vector and lies on a plane that approximately bisects the I(1)–Mo–N(1) and I(2)–Mo–N(2) angles. The metal–metal distance of 2.144 (5) Å is consistent with the description of this bond as a quadruple one and is essentially equal to those in many analogous compounds.[44] The molecular geometry also resembles that of the other $Mo_2X_4L_4$ compounds of molybdenum(II), the coordination spheres around each metal describing a square plane, with the two planes being twisted by only 4.2° away from the eclipsed configuration (the lower the twist angle, the stronger the $\delta$ component of the quadruple bond[44]). The bending of the M–ligand bonds away from the square-planar configuration around the metal to a distorted-pyramidal geometry, with the metal occupying its vertex, is also quite typical of this class of compounds and alleviates the van der Waals repulsion between the eclipsed ligands that are bonded to the adjacent metals. The iodide ligands bend more [I(1)–Mo–I(2) = 140.6 (2)°] than the nitrile ligands [N(1)–Mo–N(2) = 162.0 (1)°]. This may be attributed to the greater bulk of the iodide ligand and perhaps to the presence of a $\pi$ component in the Mo–N bonds, which would be maximized for a N–Mo–N angle of 180°. The corresponding angles in $Mo_2I_4(PMe_3)_4$, for instance, are the following: I–Mo–I = 132.35 (3)°; P–Mo–P = 150.60 (9)°.[13a,25]

**Acknowledgment.** We are grateful to the National Science Foundation for support of this work. We also thank Prof. J. L. Dye of Michigan State University for the variable-temperature magnetic susceptibility study on $Mo_3HI_7(THF)_3$·THF and Dr. X. Feng and M. P. Diebold for help with the Fenske–Hall calculations. We are indebted to Dr. Larry R. Falvello for invaluable crystallographic advice.

**Supplementary Material Available:** Tables of bond distances, bond angles, and anisotropic displacement parameters for compounds **2–7** and listings of Fenske–Hall MO energies, with the percent contribution from different kinds of atoms, for $Mo_3I_7L_3$ and $Mo_3HI_7L_3$ (L = $H_2O$, HCN) (31 pages); listings of observed and calculated structure factors for compounds **2–7** (45 pages). Ordering information is given on any current masthead page.

(38) Brencic, J. V. *Z. Anorg. Allg. Chem.* **1974**, *403*, 218.
(39) Brencic, J. V.; Leban, I. *Z. Anorg. Allg. Chem.* **1978**, *445*, 251.
(40) Cotton, F. A.; Duraj, S. A.; Powell, G. L.; Roth, W. J. *Inorg. Chim. Acta* **1986**, *113*, 81.
(41) Atwood, J. L.; Smith, K. D. *J. Chem. Soc., Dalton Trans.* **1974**, 921.
(42) Handlowic, M.; Miklos, D.; Zikmund, M. *Acta Crystallogr., Sect. B: Struct. Crystallogr. Cryst. Chem.* **1981**, *B37*, 811.
(43) Cotton, F. A.; Poli, R. *Inorg. Chem.* **1987**, *26*, 3310.
(44) Cotton, F. A.; Walton, R. A. *Multiple Bonds between Metal Atoms*; Wiley: New York, 1982.